Mathematical modeling of treatment resistance in cancer

Emilia Kozłowska

Research Program in Systems Oncology,
Research Programs Unit
Biochemistry and Developmental Biology
Faculty of Medicine
University of Helsinki
Finland

Academic dissertation

To be publicly discussed, with the permission of
the Faculty of Medicine of the University of Helsinki,
in Biomedicum Helsinki 1, Lecture Hall 3, Haartmaninkatu 8, Helsinki,
on 24th May 2019, at 12 o'clock noon.

Helsinki 2019

Supervisor

Sampsa Hautaniemi, DTech, Professor
Genome-Scale Biology Research Program, Medicum
Faculty of Medicine,
University of Helsinki
Helsinki, Finland

Reviewers appointed by the Faculty

Kalle Parvinen, Adjunct Professor
Faculty of Science and Engineering,
University of Turku
Turku, Finland

Andre Ribeiro, Professor
BioMediTech Institute,
Tampere University of Technology
Tampere, Finland

Opponent appointed by the Faculty

Sébastien Benzekry, PhD
Institut National de Recherche en Informatique et en Automatique,
Team MONC
Bordeaux, France

ISBN 978-951-51-5194-0 (paperback)
ISBN 978-951-51-5195-7 (PDF)
`http://ethesis.helsinki.fi`
Unigrafia Oy
Helsinki 2019

to my family and friends

All models are wrong but some are useful
George E. P. Box

Abstract

Cancer is one of the world's most lethal diseases. Although our understanding of this disease is expanding continuously, treatments for many types of cancers are still insufficient. The main reason for the high mortality of cancer patients is resistant to therapy. Since resistance to therapy is a complex and dynamical process, an interdisciplinary approach is necessary to understand it.

The emergence of a new field called integrative mathematical oncology can tackle many urgent clinical problems in the treatment of cancer that are impossible to address using, for example, an *in vitro* or *in vivo* approach. The primary goal of this new field is to translate the biological complexity of a tumor into a precise language, such as mathematical formulas, and to perform model simulations. Therefore, integrative mathematical oncology allows for biological experiments to be performed inexpensively and rapidly.

This thesis applies the integrative mathematical oncology (IMO) approach to investigate resistance to treatment in solid tumors at the molecular and cellular levels. A mathematical model of the most commonly dysregulated pathway in cancer (the p53 signaling pathway) underwent a bifurcation analysis to investigate the possibility of restoring its proper dynamics in two types of cancer: osteosarcoma and breast cancer. Next, a stochastic model of resistance to platinum compounds was developed to improve our understanding of chemo-resistance to this group of drugs in advanced high-grade serous ovarian cancer (HGSOC). Finally, virtual clinical trial simulations (VCTS) were performed to identify a novel drug combination in ovarian cancer.

The application of integrative mathematical oncology deepened our understanding of radio- and chemo-resistance in solid tumors. Firstly, the results from the bifurcation analysis of the p53 signaling pathway suggested silencing Mdm2 using siRNA to overcome radio-resistance in breast cancer and osteosarcoma. Next, the stochastic model of platinum resistance was utilized to answer two urgent clinical questions about ovarian cancer: i) how many platinum resistance mechanisms are active at diagnosis, and ii) how many drug-resistance mechanisms must be targeted to improve patient outcomes. Finally, the clinical trial simulations suggested a novel drug combination to overcome platinum resistance in advanced high-grade serous ovarian cancer.

Streszczenie

Rak jest jedną z najbardziej śmiertelnych chorób na świecie. Pomimo tego, że wiedza na temat tej choroby jest ciągle rozwijana, terapia w przypadku wielu typów nowotworów jest nieefektywna. Głównym powodem wysokiej śmiertelności pacjentów chorych na raka jest oporność na terapię. Jakoże oporność na terapię jest skomplikowanym i dynamicznym procesem, interdyscyplinarne podejście jest niezbędne do jego zrozumienia.

Pojawienie się nowej dziedziny zwanej zintegrowaną matematyką onkologiczną jest w stanie rozwiązać wiele ważnych problemów klinicznych, które są niemożliwe do rozwiązania przy użyciu *in vitro* lub *in vivo*. Głównym celem tej nowej dziedziny jest przetlumaczenie biologicznej złożoności nowotworów na precyzyjny język, taki jak formuły matematyczne, i wykonanie symulacji modelów. Dlatego zintegrowana onkologia matematyczna umożliwia wykonanie eksperymentów biologicznych szybko oraz bez dużych nakładów finansowych.

W tej pracy, podejście matematyki onkologicznej zostało wykorzystane do zrozumienia oporności zbitych nowotworów na leczenie w dwóch skalach: molekularnej i komórkowej. Najpierw, model matematyczny najbardziej rozregulowanej ścieżki sygnałowej w raku (ścieżce sygnałowej p53) został poddany analizie bifurkacji celem zbadania możliwości przywrócenia prawidłowej dynamiki tej ścieżki sygnałowej w dwóch nowotworach: kostniakomiessakach i nowotworach piersi. Następnie, stochastyczny model lekooporności na platynę został wykonany celem zrozumienia mechanizmów lekoopornosci na platynę w zaawansowanym surowiczym raku jajnika. Na koniec, virtualne symulacje prób klinicznych zostały wykonane celem zidentyfikowania nowych kombinacji leków w raku jajnika

Zasosowanie zintegriwanej matematyki onkologicznej pogłębiło naszą wiedzę o opornosci na radio- i chemo-terapię w nowotworach zbitych. Najpierw, wyniki z analizy bifurkacyjnej ścieżki sygnałowej p53 proponuje wyciszenie Mdm2 przy użyciu siRNA celem pokonania radiooporności w raku piersi i kostniakomięsaku. Następnie, stochastyczny model opornosci na platynę został wykożystany celem odpowiedzi na dwa pilne pytania kliniczne: i) ile mechanizmów oporności na platynę jest aktywnych podczas diagnozy i ii) ile mechanizmów lekoopornosci na platynę nalezy celować celem poprawy przeżywalności. Na koniec, symulacje prób klinicznych sugerują nową kombinację leków celem pokonania lekooporności na platynę w surowiczym raku jajnika.

Contents

Abbreviations

^{18}F–FDG	^{18}F-fluorodeoxyglucose
ABC	ATP-binding cassette transporter
ADJ	adjuvant chemotherapy
BIC	Bayesian information criterion
Ctr1	cooper transporter 1
CNV	copy number variations
CSC	cancer stem cell
DS	drug delivery system
DOX	doxorubicine
GSH	glutathione
GOF	goodness of fit
G–W model	Galton–Watson model
GSA	global sensitivity analysis
HGSOC	high–grade serous ovarian cancer
IDS	interval debulking surgery
IR	ionizing radiation
IMO	integrative mathematical oncology
ITH	intratumor heterogeneity
K–M plot	Kaplan–Meier plot
LHS	latin hybercube sampling
LSA	local sensitivity analysis
M–C method	Monte–Carlo method
MDR	multidrug resistance
MTD	maximum tolerated dose
MTV	metabolic tumor volume
NCCN	National Comprehensive Cancer Network
NACT	neoadjuvant chemotherapy
ODE	ordinary differential equations
PARPi	PARP inhibitor
PDS	primary debulking surgery
PET/CT	positron emission tomography / computed tomography
PFI	platinum–free interval
PRCC	partial rank correlation coefficient
RMSE	root mean squared error
SA	sensitivity analysis
SMI	small molecule inhibitor
SOC	standard of care
SSA	stochastic simulation algorithm
S_t	survival probability at given time
TCGA	the Cancer Genome Atlas
TUH	Turku University Hospital
VCTS	virtual clinical trial simulation

Publications and author's contributions

This thesis comprises of an introductory review and three publications. In the text, these publications are referred to as Publication I, Publication II, and Publication III.

Publication I **Emilia Kozłowska**, Krzysztof Puszynski.
Application of bifurcation theory and siRNA-based control signal to restore the proper response of cancer cells to DNA damage.
Journal of Theoretical Biology, 2016,408:213-21.
doi: 10.1016/j.jtbi.2016.08.017

Publication II **Emilia Kozłowska**, Anniina Färkkilä, Tuulia Vallius, Olli Carpén, Jukka Kemppainen, Seija Grénman, Rainer Lehtonen, Johanna Hynninen, Sakari Hietanen, Sampsa Hautaniemi.
Mathematical modeling predicts response to chemotherapy and drug combinations in ovarian cancer.
Cancer Research, 2018, 78(14) 4036-4044.
doi:10.1158/0008-5472.CAN-17-3746.

Publication III **Emilia Kozłowska**, Tuulia Vallius, Johanna Hynninen, Sakari Hietanen, Anniina Färkkilä, Sampsa Hautaniemi.
Virtual clinical trials identify effective combination therapies in ovarian cancer.
Submitted.

Author's contributions

Publication I Designed the study, performed model simulations, performed bifurcation analysis, and wrote the paper.

Publication II Designed the study, analyzed clinical data, developed mathematical model, performed all model simulations, and wrote the paper.

Publication III Designed the study, developed mathematical framework, performed clinical trial simulations, and wrote the paper.

1 Introduction

Cancer's key trait is the disruption of the balance between cell proliferation and cell death, resulting in uncontrolled tumor growth, invasion, and metastasis. Cancer is a complex disease in which (epi)genetic alternations occur at the subcellular level and lead to functional changes at the cellular and tissue levels. Therefore, cancer is believed to be a multi-scale process where understanding each scale and connection between them requires a holistic approach, such as data-driven mathematical modeling [1].

Applying mathematics to oncology is relatively new. The field aims to describe cancer on multiple levels, such as the molecular and cellular levels, using mathematical formulas [2]. A constructed model can be then analyzed using mathematical methods, or simulated numerically to improve our understanding of cancer and suggest novel treatment modalities. As more and more omics and clinical data are collected, mathematical models of cancer can be calibrated and validated leading to more accurate results from model simulations. Moreover, recent advancements in mathematics and availability of high computing power allow for the simulation of complex individual-based and multiscale models [3, 4]. As a result, a new subfield of oncology called integrative mathematical oncology (IMO) has emerged [5].

IMO is at the intersection of mathematics and oncology where the goal is to understand cancer from a mechanistic viewpoint [6]. By translating the biological complexity of such a complex disease into mathematical language, IMO describes cancer-related phenomena through an emerging outcome that is predicted by model simulations. IMO can be divided into two subfields: computational and physical one [7]. The first one uses high-throughput data, such as genomics or proteomics, to build models that can quantitatively predict the patient's outcome. For instance, the phylogenetic model of tumor evolution can be constructed to understand the evolution of tumor progression [8]. Physical oncology, which is the focus of this thesis, views cancer as a complex biological system and aims to create mechanistic models of tumorigenesis and cancer progression. This subfield contributes for example to the understanding of treatment resistance in cancer, among other things [9].

IMO approach has been applied to answer a wide range of questions in oncology. For example, it was used to investigate the effectiveness of cancer screening [10], suggest novel drug combinations [11], understand complex interactions in the tumor microenvironment [12], suggest more optimal drug scheduling [13], and estimate the probability of metastasis [14]. However, IMO is still an emerging field and only a few mathematical models have been translated into clinical practice successfully

[15].

This thesis aims to suggest novel methods to overcome resistance to therapy in solid tumors using integrative mathematical oncology approach. The thesis focuses on radio- and chemo-sensitivity on the molecular and cellular levels. First, a model of the p53 signaling pathway for two types of cancer (osteosarcoma and breast cancer) is developed to investigate resistance to ionizing radiation (IR). The results of the model analysis suggest silencing Mdm2 as a means to overcome radio-resistance. Next, a model of resistance to platinum compounds is developed and applied to find a method to revert resistance to platinum-based chemotherapy in advanced HGSOC. Finally, virtual clinical trials simulations are employed to test the effectiveness of combining platinum with drugs that target specific platinum-resistance mechanisms.

2 Cancer

In order to survive, all living organisms require constant maintenance of stability called homeostasis. In human body, blood pressure, blood sugar, oxygen, pH, and temperature, among other things, are constantly being adjusted to maintain a constant level. It means the human body is in a constant dynamic equilibrium [16]. Disruption of this mechanism leads to various diseases, such as cancer.

In order to maintain homeostasis, the number of cells in the adult human body is kept constant, and cell division usually occurs to replace dead cells [17]. This process is controlled in the cell through the regulation of cellular growth and death signals. An imbalance between the signals to divide and die can lead to carcinogenesis. Therefore, on the most basic level, cancer can be defined as a disease of uncontrolled cell growth and cell division [18].

Cancer is not a single disease, but rather, a group of disorders that can be divided by type of origin tissue (histology) or location in the body (primary site) [19]. The National Cancer Institute defines over 200 types of cancer [20], and the most common type (80% of all cancer cases) is epithelial one [21].

Tumors are usually divided into two categories: solid and hematological malignancy. Solid tumors, which are the focus of this thesis, are defined as abnormal clumps of cells that typically do not contain liquids or cysts [22]. Hematological cancers, instead, usually do not form a tumor. Instead, they originate in the blood, bone marrow, or lymphatic system and include leukemia, lymphoma, and myeloma.

2.1 Ovarian cancer

In 2018, 295,414 of new ovarian cancer cases were diagnosed, and 184,799 women died [23]. Ovarian cancer is the eight most common cancer in women and ranks as the fifth cause of deaths related to cancer among women. Ovarian cancer has a high mortality rate because it is usually diagnosed at advanced stages due to the absence of accurate screening methods and also unspecific symptoms in the early stage [24].

Ovarian cancer is a disease that originates from the epithelial, germ, or stromal cell [25]. Epithelial ovarian cancer is the most common subtype of ovarian cancer and constitutes 95% of all cases [26]. Two-thirds of all epithelial tumors are serous and can be divided into two groups: low-grade (10%) and high-grade (90%). Therefore, HGSOC, which is the focus of this thesis, is the most common subtype of ovarian cancer, accounting for approximately 70% of all ovarian cancer cases [27].

High grade serous ovarian cancer is not a single disease, but rather a family of non-uterine ovarian cancers originating from an epithelial cell [28, 29]. It is the most aggressive histological subtype of ovarian cancer. Although the five–years survival of early-stage patients is higher than 80%, the advanced HGSOC has the five–years survival rate below 30% [30]. HGSOC is characterized by a mutation in the *p53* gene, high genomic instability, the high number of DNA copy number variations, and few somatic mutations [31].

2.1.1 Standard of care in HGSOC

The first–line treatment for ovarian cancer depends on tumor stage, dissemination to other organs, and patient's physical condition. This section describes the standard treatment protocol for newly diagnosed advanced ovarian cancer following the current clinical practice guidelines [32, 33]. Figure 1 presents a schematic of the standard of care (SOC).

When ovarian cancer is suspected, two types of clinical assessment are performed: blood tests to measure cancer biomarkers (such as CA-125 and HE4), and CT scans to determine if a pelvic mass is malignant. The National Comprehensive Cancer Network (NCCN) guidelines suggest using these measurements together with an algorithm called the Risk of Ovarian Malignancy Algorithm (ROMA) [34].

After diagnosing advanced ovarian cancer, a laparoscopy is performed to evaluate whether optimal cytoreduction is possible since the residual tumor burden is a key clinical parameter that correlates with patients' outcomes [35]. Optimal cytoreduction means that the residual tumor nodules have a maximum diameter of 1 cm. The patients are assigned to one of two treatment groups, as indicated in Figure 1. The first group is called the primary debulking surgery group (PDS), and the second group is called the neoadjuvant treatment group (NACT).

When optimal debulking is possible at the time of diagnosis, the patient is assigned to the PDS group where primary debulking surgery is performed to remove the ovaries, fallopian tubes, and uterus. Next, the patient undergoes at least six cycles of platinum-taxane chemotherapy administered intravenously with a three-weeks interval.

If optimal debulking is not possible, an alternative solution is administering neoadjuvant chemotherapy (NACT). Usually, three cycles of platinum-taxane chemotherapy or platinum alone are administered. After NACT, clinical evaluation is performed to check if the tumor is operable by measuring the CA-125 biomarker and performing computed tomography (CT) scans. If the tumor is operable, interval debulking surgery (IDS) is performed following another three cycles of adjuvant chemotherapy

(ADJ). If the patient is inoperable after NACT, they are referred to alternative or palliative treatment.

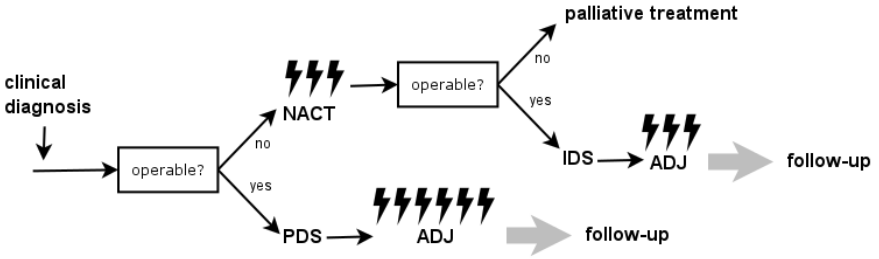

Figure 1: Schematic of primary treatment in advanced HGSOC. NACT = neoadjuvant chemotherapy; PDS = primary debulking surgery; IDS = interval debulking surgery; ADJ = adjuvant chemotherapy.

2.2 Models of carcinogenesis

One of the hallmarks of cancer is the ability of cancer cells to sustain proliferative signals [36]. Healthy cells control the release of growth-promoting signals carefully. However, cancer cells continually emit proliferative signals that permit their survival and abnormal proliferation [37]. Many theories have attempted to explain how sustaining proliferating signaling drive carcinogenesis [38]. Figure 2 presents the two most well-known theories, which are called hierarchical and the stochastic model.

The clonal evolution model (or stochastic model) assumes that cancer is initiated from a healthy cell through the accumulation of (epi)genetic changes. These changes accumulate in cancer cells, leading to the appearance of various subclones with a different spectrum of (epi)genetic aberrations. Some changes confer a selective advantage and allow the clone to out-compete other ones. This model of carcinogenesis assumes that all subclones have the potential for self-renewal. Therefore, all clones need to be targeted by a chemotherapeutic agent in order to eradicate the entire tumor [39].

Hierarchical model, the growth of the tumor is only dependent on a small fraction of cancer cells called cancer stem cells (CSCs). Cancer is initiated from a single CSC that undergoes differentiation and has the potential for self-renewal. Therefore, the tumor is assumed to be composed of a small population of CSCs that are responsible for tumor growth and a large fraction of differentiated cancer cells that have lost the potential for self-renewal. In this model, treatment only targets CSCs because they are the only cells that contribute significantly to tumor perpetuation [40].

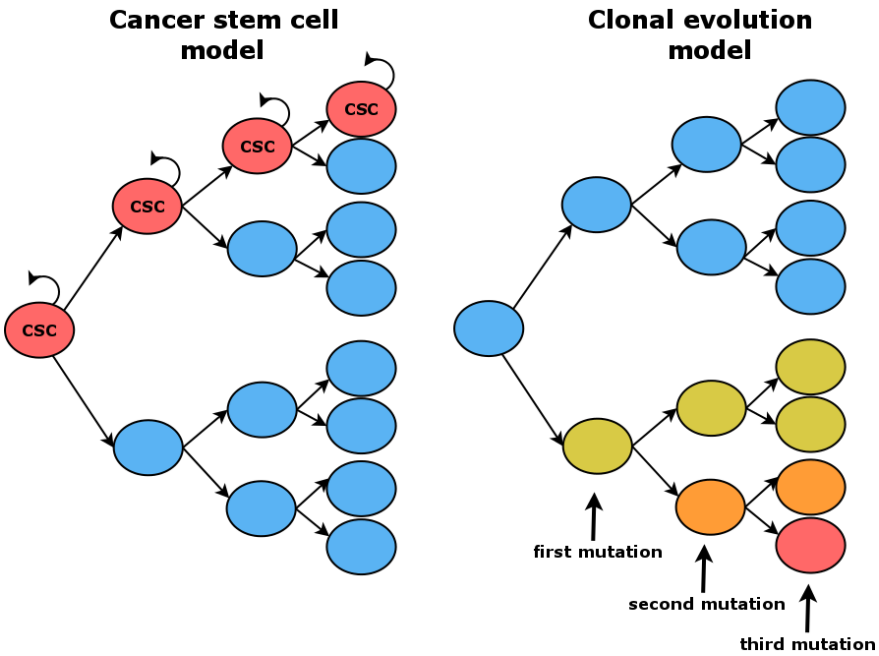

Figure 2: Two models of carcinogenesis: cancer stem cell (hierarchical) and clonal evolution (stochastic). The cancer stem cell model proposes that cancer is initiated by cancer stem cells (CSCs) that are pluripotent and self-renewing. CSCs divide unfaithfully, leading to the appearance of differentiated cells (blue). In the clonal evolution model, cancer is initiated through a cancer cell that can acquire new mutations, leading to the appearance of a new subclone. Adapted from [40].

2.3 Tumor evolution

Cancer is subjected to the same evolutionary forces, such as selection and genetic drift, like other evolutionary systems [39, 41]. Evolutionary theories about neoplasm are crucial for understanding tumor progression and the resistance to treatment, among other processes [42]. The current belief is that understanding the ecological and evolutionary properties of a tumor could help clinicians suggest better treatment strategies and predict responses to therapies [43]. Therefore, understanding tumor evolution and intra-tumor heterogeneity (ITH) are essential for improving patient survival.

The theory of cancer evolution suggests that carcinogenesis is a multi-stage process with three major steps: initiation, promotion, and progression (see Figure 3). In the first phase, (epi)genetic alternations are acquired by a healthy cell, leading to the appearance of a tumor-initiating cell. The process is called tumor initiation. Next, tumor promotion leads to selective clonal expansion of tumor-initiating cells and the production of a large population of pre-neoplastic cells that become at risk of

conversion. The last phase of multistage carcinogenesis is tumor progression. Here, a tumor cell arises and divides into malignant cells which initially form a benign tumor and then spread to distant organs through a process called metastasis.

As a result of evolutionary forces, a tumor composes of many types of cancer cells (subclones) that have accumulated different (epi)genetic aberrations, leading to ITH. It is why, even though, the administration of first-line therapy to the tumor, often leads to a successful reduction of its mass, the same treatment also applies Darwinian selection for drug-resistant clones. Therefore, it is suggested that the aim of cancer treatment should not be to remove as many cancer as possible in a short timeframe, but rather treatment should focus on targeting drug-resistant subclones [44].

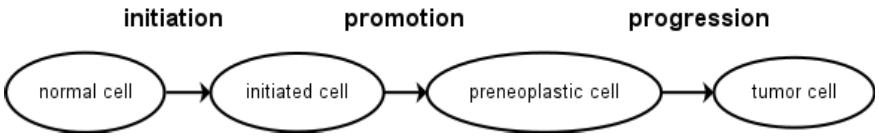

Figure 3: Multistage tumorigenesis.

2.4 Cancer treatment

Cancer can be treated using various strategies, including surgery, chemotherapy, radiotherapy, and targeted therapy. The type of treatment depends on the tumor's location, stage, and the patient's overall condition. Treatments can be administered in combination. For example, for advanced HGSOC patients, surgery and chemotherapy are used as a first-line treatment [45].

The current paradigm considers cancer a local disease that sometimes later spreads to distant organs [46]. Based on this paradigm, it is suggested that the primary treatment of solid tumors should include surgery. Therefore, removal of tumor cells could cure the patient, if cancer has not spread to other organs. Indeed, surgery is a key treatment intervention for breast and ovarian cancer [47, 48].

Chemotherapy involves the administration of chemicals to inhibit the growth of malignant cells. The rationale behind chemotherapy is that fast-dividing cancer cells are more sensitive to DNA damage and, therefore, most prone to chemotherapy-induced death [49]. The goal of chemotherapy depends on the stage of the tumor and the patient's general condition. For example, induction chemotherapy is administered as a first-line treatment to cure the patient, while consolidation chemotherapy is administered after remission to prolong the patient's survival [50].

Targeted therapy is one of the most commonly applied strategies in cancer treatment

nowadays, and targets the molecules needed for carcinogenesis and tumor growth rather than focusing on fast-dividing cells [51]. There are two major types of targeted-therapy drugs: one blocks the actions of specific proteins involved in spreading cancer (e.g., PARPi in ovarian cancer) [52] and the other targets the immune system to kill cancer cells (e.g., PD-L1 inhibitors in ovarian cancer) and is called immunotherapy [53]. The goal of targeted therapy is to specifically target cancer cells without affecting healthy cells.

Radiotherapy is a type of treatment that uses a high dose of radiation (e.g., X-rays or gamma rays) to kill cancer cells [54]. There are two ways to administer radiotherapy: external beam radiation therapy and internal radiation therapy. High-energy ionizing radiation (IR) damages DNA, thus blocking the ability of cancer cells to divide. Radiotherapy kills both healthy and cancer cells, but cancer cells are less proficient at repairing DNA damage caused by IR.

3 Treatment resistance in cancer

Administering chemotherapeutic drugs, such as cisplatin, shows excellent initial response [55, 56]. However, after a short time, tumor recurrence is often observed with the tumor resistant to chemotherapy. As a result, multi-drug resistance (MDR) emerges. Therapy resistance can be divided into two major groups: intrinsic (pre-existing) and acquired [57]. Intrinsic therapy resistance means that mediating factors, such as mechanical or biochemical factors, existed in the tumor before the treatment was administered. Alternatively, acquired therapy resistance develops during treatment as a result of (epi)genetic aberrations in tumors that were initially sensitive to therapy [58]

Figure 4 presents the two main mechanisms of therapy resistance, which are alternations in the drug metabolism and modifications to the drug target [59]. The next section describes both mechanisms of therapy resistance.

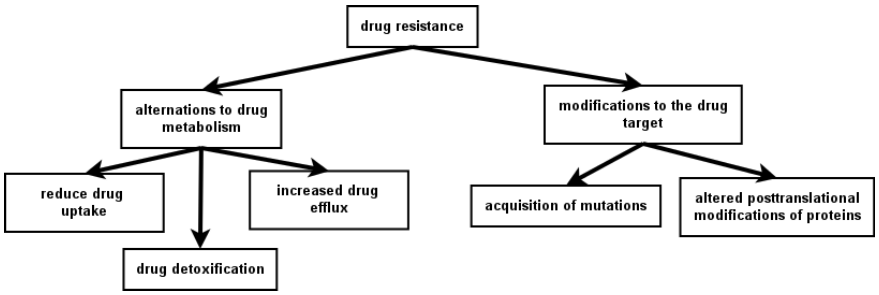

Figure 4: Mechanism of drug resistance to chemotherapy in cancer. Adapted from [59].

3.1 Types of treatment resistance in cancer

The most widely studied mechanisms of drug resistance are those caused by alternations in drug metabolism. These alternations can be divided into three categories: reduced drug uptake, drug detoxification, and increased drug efflux.

Transport of chemotherapeutic drugs (driven mostly by cell receptors) depends on its chemical properties. Resistance can be caused by mutations that modify the activity of cell receptors or transporters, such alternations in the copper transporter receptor 1 (CTR1) in ovarian cancer [60]. The second mechanism of drug resistance is caused by aberrations in metabolism due to increased drug efflux. For instance, increased expression of the ATP-binding cassette (ABC) membrane transporters correlates with resistance to doxorubicin [61]. Finally, drug deactivation can happen

before it binds to its target. For example, glutathione (GSH) is shown to inactivate platinum drugs [61].

Modification of a drug target is another type of drug resistance in cancer. The effectiveness of a specific drug depends on its ability to bind to its target, such as DNA. Mutations in the drug target could lead to the production of a protein with a modified binding site. Therefore, binding becomes impossible, even if the drug reaches its target. For instance, PARP inhibitors (PARPi) are administered to treat ovarian cancer patients with a mutation in *BRCA1/2*. However, a spontaneous mutation could reverse the original mutation in this gene, leading to drug resistance [62].

In addition to the cellular mechanisms of treatment resistance, non-cellular ones are also observed, especially in solid tumors [63]. These non-cellular mechanisms involve interactions between cancer cells and a different component in the tumor microenvironment. For instance, response to chemotherapy is influenced by the vasculature since chemotherapeutic drugs gain access to tumor cells via the blood vessels. It is known that blood-flow in a tumor is variable and disorganized, which results in a hypoxic region where the drug cannot enter [64].

3.2 Methods to overcome treatment resistance in cancer

To overcome drug resistance in cancer patients, drug scheduling and chemotherapeutic agents are usually changed. However, these approaches cannot always be applied because patients gain drug resistance to multiple agents over time, leading to MDR. This section discusses the most common strategies for overcoming drug resistance in cancer patients.

The first method to re-sensitize cancer cells to treatment is to find analogs to one of the most widely administered chemotherapeutic agents. For instance, doxorubicin (DOX) is a compound that is applied during the treatment of many solid tumors [65] because it is one of the most effective chemotherapeutic agents. Therefore, extensive work has been done to find an analog of DOX, such as epirubicin, which is less toxic and does not lead to drug resistance [66].

The second strategy for reversing therapy resistance is administering chemosensitizers together with standard treatment. The most important mechanism of MDR is overexpression of ABC transporters, which are responsible for low-drug bioavailability by pumping the drug out of the cells. Verapamil was the first chemosensitizer approved by the FDA to target ABC transporters [67].

The third method for addressing a treatment-resistant tumor is so-called targeted therapy, which targets specific signaling pathways that are upregulated in resistant

tumor using, for example, small molecule inhibitors (SMIs). SMIs are small molecules (around 500 Da) that block the activity of key molecules and, thus, suppress the proliferation and differentiation of tumor cells [68]. For instance, NSC23925 SMI is an effective inhibitor of P-glycoprotein (also known as MDR1 protein) in ovarian cancer. Recent studies have shown that NSC23925 could prevent resistance to paclitaxel in ovarian cancer [69].

The application of delivery systems is the fourth method to target resistance to treatment in a cancer patient. One of the goals of these systems is to increase drug concentration, especially in solid tumors, by relying on vascular permeability and ineffective lymphatic drainage. One example of nanomedicine that has been approved by the FDA [63] is Doxil (PEGylated liposomal Dox), which encapsulates DOX and delivers it to the tumor using a vesicle called liposome.

4 Mathematical models of treatment resistance in cancer

Many computational tools are available to model treatment resistance in cancer. These can be divided into two groups: i) mechanistic modeling and ii) data-driven predictive modeling [70]. The first group is comprised of dynamical models that describe mechanisms of therapy resistance from a molecular or cellular point of view whereas data-driven predictive modeling applies various omics data to create a probabilistic model to identify for example biomarkers for treatment resistance.

This thesis focuses on the development of a mechanism-based mathematical model. A kinetics model of the p53 signaling pathway was developed to study radio-resistance in a solid tumor, and a stochastic model of platinum resistance in ovarian cancer was created to investigate mechanisms of platinum resistance in HGSOC.

The main focus of this thesis is stochastic modeling of platinum resistance in HGSOC; therefore, this chapter discusses stochastic models of tumor evolution following description of two models of chemotherapy.

4.1 Models of treatment resistance evolution in cancer

The accumulation of various random (epi)genetic aberrations is one of the reasons for resistance to cancer treatment. Therefore, stochastic mathematical models are powerful mathematical tools to study treatment resistance. Stochastic models of evolution can be for example in form of: i) the Moran model, ii) the Wright-Fisher model, and iii) the branching model [71]. Figure 5 presents a schematic of these three models.

4.1.1 Constant population size models

The Moran and Wright-Fisher models both assume a constant population size. This means that the number of cells is constant during the entire course of the simulation. Such models have been widely applied to study the effects of various evolutionary forces, such as genetic drift and natural selection [72]. Both models are discrete-time models, which means the state of the system is updated at finite, constant time intervals.

The Moran process model assumes that generations overlap and the population size

remains constant, N, with m different types of cells [73]:

$$N = \sum_{i=1}^{m} N_i,$$

where N_i is the number of cells in subclone i. Each subclone can have a different fitness value $f_1, f_2 \dots f_m$. During each time step, one cell of type i is chosen to divide with a probability that is proportional to its fitness value, f_i. Subsequently, a random cell is chosen to die, and to be replaced by another cell, chosen from with probability influenced by its selective value, which leads to the following equation, which describes the probability that cell type i increases and cell type j decreases [71]:

$$P(N_i \to N_i + 1, N_j \to N_j - 1) = \frac{N_i \cdot f_i}{\sum_{k=1}^{m} N_k \cdot f_k} \frac{N_j}{N}.$$

The major drawback of the Moran process model is that the model is computationally expensive to simulate. Modification of the Moran process model, called the Wright-Fisher model, was proposed [74, 75]. In contrast to the Moran process, the Wright-Fisher model samples the whole population with a probability distribution in every generation; therefore, the model assumes that generations do not overlap.

Wright–Fisher model involves sampling with replacement from the population at generation t to derive the population at generation at $t+1$. Assuming the simplest scenario with two types of cells, N_i and N_j cells, and given a total population size N, the probability of cell type i contain N_{ii} cells at the next generation follows the binomial distribution:

$$P(N_i \to N_{ii}) \approx Bin(N_{ii}; N, \frac{N_i \cdot f_i}{\sum_{k=1}^{m} N_k \cdot f_k}).$$

The Moran process and the Wright-Fisher model are related to each other. One generation of the Wright-Fisher model equals n generations of the Moran process, and both models lead to similar results. For example, fixation probabilities are almost identical in both models. Although the Moran process model has the benefit of more accurate analyses, the Wright-Fisher model is much more efficient from a computational perspective.

4.1.2 Fluctuating population size model

The most widely applied model with a fluctuating population size is the branching process model [76]. It is a Markov process model where each individual produces offspring with rate λ during time-interval between t and $t + \Delta t$ independently of other individuals. In the simplest scenario, one of three processes is possible at a

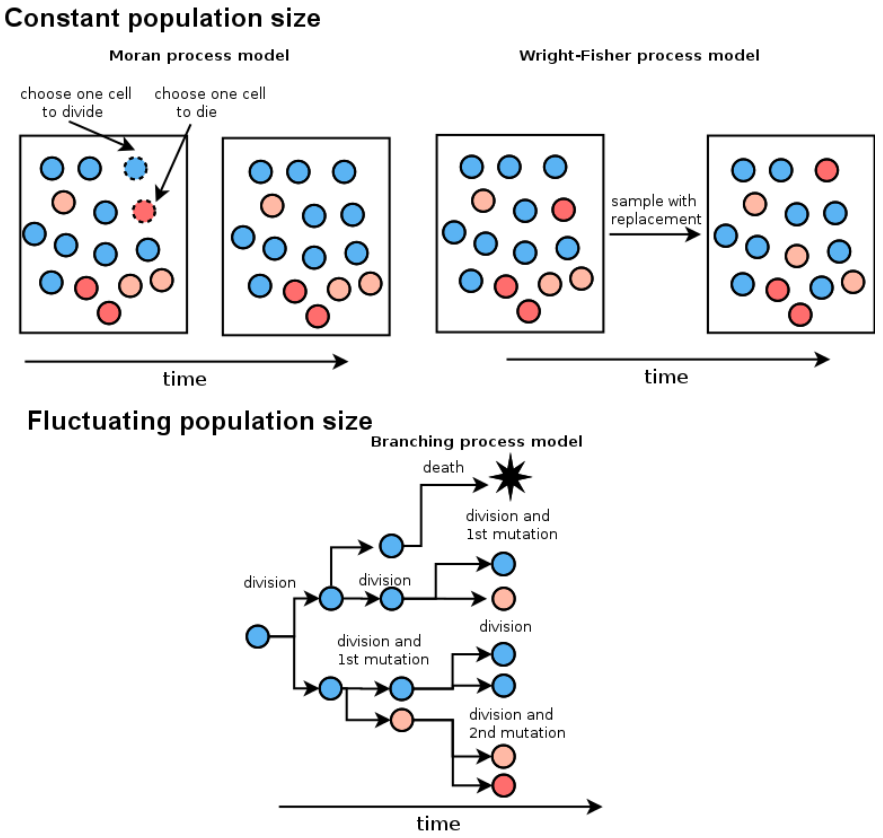

Figure 5: Mathematical models of drug resistance evolution. Three models of evolution are presented in the Figure: Moran process, Wright—Fisher, and branching process model (Adapted from [71].

given time-interval: i) division without mutation (symmetric division) with rate $\lambda(1-u)$, ii) cell death with rate d, and iii) division with a mutation leading to the emergence of a new type of cell with mutation rate $\lambda \cdot u$ (asymmetric division). The rate of each event is independent of population composition and size.

In case of two type of individuals (A and B), the probability of each event after very short time interval Δt is given with the following equations:

$$P(N_a+1(t+\Delta t);N_b(t+\Delta t)|N_a(t),N_b(t)) = \lambda(1-u)N_a(t)\Delta t + \lambda u N_b(t)\Delta t$$

$$P(N_a(t+\Delta t);N_b+1(t+\Delta t)|N_a(t),N_b(t)) = \lambda(1-u)N_b(t)\Delta t + \lambda u N_a(t)\Delta t$$

$$P(N_a-1(t+\Delta t);N_b(t+\Delta t)|N_a(t),N_b(t)) = d\cdot N_a(t)\Delta t$$

$$P(N_a(t+\Delta t);N_b-1(t+\Delta t)|N_a(t),N_b(t)) = d\cdot N_b(t)\Delta t$$

where N_a and N_b is number of individuals in a subclones A and B, respectively.

The branching process is a powerful tool for modeling the stochastic growth of a tumor assuming exponential tumor growth. The model was applied to answer various urgent questions in oncology such as i) What is the probability of metastasis of pancreatic cancer [77], ii) What is the selection advantage of somatic mutations in cancer [78], and iii) What is the probability of intrinsic resistance to ibrutinib in chronic lymphocytic leukemia [9].

4.2 Modeling chemotherapy treatment

The mathematical models presented in the previous section consider unperturbed tumor growth without treatment intervention. However, it is also important to model tumor dynamics under treatment, especially when attempting to model acquired drug resistance in cancer patients. This section reviews two of the most common models for chemotherapy that could be combined with models of tumor growth.

Skipper–Schabel model

The oldest model of chemotherapy is the Skipper-Schabel model, which is known as the log–kill hypothesis [79]. This hypothesis states that when the tumor grows exponentially (increasing in size by a constant fraction every fixed-time interval), the tumor also shrinks by a constant fraction called log-kill in the presence of chemotherapy. This model can be defined with the following equation:

$$\dot{N}(t) = \lambda \cdot N(t) - C \cdot N(t),$$

where λ is growth rate and C is drug concentration.

The Skipper-Schabel model is also known as the second Skipper law, which states that the fraction of cells killed by a given drug dose is constant (independent of tumor burden); therefore, a linear increase in dose size causes a log increase in the cell kill rate [80]. For example, if drug dose C shrinks the tumor size from 10^{10} cells to 10^9 and kills 90% of cells (one-log kill), the same dose will reduce the tumor burden from 10^9 to 10^8.

Norton–Simon model

The log-kill model assumes that tumors grow exponentially. While this assumption is valid for liquid tumors, the growth dynamics of solid tumors follow Gompertzian

growth dynamics. Norton and Simon developed the following model to describe chemotherapy in solid tumors:

$$\dot{N}(t) = f(N(t))(1 - C(t)),$$

where $f(N(t))$ represents the growth dynamics of unperturbed tumor growth rate and $C(t)$ is drug concentration.

Norton–Simon formulated the following hypothesis of chemotherapy treatment based on the above model: "Therapy results in a rate of regression in tumor volume that is proportional to the rate of growth that would be expected for an unperturbed tumor of that size."[81]

L. Norton and R. Simon developed a hypothesis that is now the basis for a novel strategy in cancer treatment called dose-dense chemotherapy [81]. Based on this theory, smaller tumors grow faster and are, thus, simpler to eradicate than a large tumors. Therefore, L. Norton and R. Simon suggest that the best way to eliminate all tumor cells is to administer chemotherapy with the same dose but more frequently than standard chemotherapy in order to minimize the risk of tumor regrowth between chemotherapy cycles. This hypothesis was successfully validated in the clinical trial 20 years later [82].

5 Mathematical model analysis

After constructing and calibrating the model, the next crucial step is analyzing its behavior. Model analysis is an integral part of the modeling process. This section reviews two of the most common methods for model analysis: sensitivity and bifurcation analyses.

5.1 Sensitivity analysis

Estimating the precise parameter values for a mathematical model is one of the challenges of mathematical modeling. The lack of precise values can be addressed by performing a sensitivity analysis (SA) that allows for the quantification of uncertainty in the model outputs.

There are three main applications of SA, and the most important is model development. SA is applied extensively to guide parameter estimation and check the correctness of the model's assumptions [83]. The second application of SA is the reduction of a mathematical model [84]. The major challenge of systems biology is to reduce the mathematical model defined with hundreds of equations in order to perform model simulations in an acceptable amount of time with limited memory while preserving the qualitative model behavior. The third application of SA is finding parameters that are sensitive to the output. For example, SA can facilitate searching for new drug targets in cancer or optimize the drug dose and schedule by checking the model parameters that most affect output, such as overall survival [85].

SA can be divided into two types: local SA (LSA) and global SA (GSA). The LSA involves perturbing the nominal parameter value by a small amount and calculating the effect it has on the output. The GSA method requires changing the parameter values over a wide range to assess its impact on the model output.

5.1.1 Local methods

Some mathematical models can be described as a system of ordinary differential equations:

$$\frac{dy_i}{dt} = f_i(y_i, p, t) \quad i = 1, 2, \ldots, n,$$

where y_i is a vector of variables and p is a vector of model parameters. The effect of a small parameter change can be expressed as a Taylor series expansion:

$$y_i(t, p+\Delta p) = y_i(t,p) + \sum_{j=1}^{m} \frac{\partial y_i}{\partial p_j}\Delta p_j + \frac{1}{2}\sum_{l=1}^{m}\sum_{j=1}^{m} \frac{\partial_i^2}{\partial p_l p_j}\Delta p_j p_l + \ldots$$

where the first–order local sensitivity coefficient equals $\frac{\partial y_i}{\partial p_j}$ and form sensitivity matrix:

$$S(t) = \{s_{ij}\} = \{\frac{\partial y_i}{\partial p_j}\}$$

The sensitivity coefficient describes the effect on the i^{th} output as a result of a small change in the j^{th} parameter around its nominal value. The sensitivities coefficients can be approximated using the finite difference method (indirect method) where sensitivity coefficients are given in the following formula:

$$s_{ij} \approx \frac{y_i(p_j + \Delta p_j, t) - y_i(p_j, t)}{\Delta p_j}$$

In this method, the model is solved at the nominal parameters values and then at some perturbed value of parameter p_j while the other parameters are kept at theirs original values.

5.1.2 Global methods

LSA is applied to study the model outcome in the neighborhood of nominal parameter values, i.e., locally. However, the values of the model parameters can vary widely in biological systems. Therefore, a global sensitivity analysis is applied to quantify the model sensitivity for a wide range of input parameters [86].

The simplest global SA methods are based on sampling. The sampling–based methods use Monte–Carlo (MC) techniques to investigate the relationship between model inputs and outputs. For a model with m inputs $p = \{p_1, p_2 \dots p_m\}$ a sampling method consists of three steps:

1. Generate N values of parameter p_i from given probability distribution,
2. Evaluate the model for each element in the input sample and extract model outputs,
3. Quantify and map inputs with outputs.

The most popular sampling method applied in GSA is Latin hypercube sampling (LHS). GSA requires that the entire input space is sampled appropriately, which requires a large number of samples. This becomes a problem when the model requires intensive computational simulation. Thus, the LHS method was proposed as a more efficient way to sample inputs from the probability distribution [87]. In one-dimensional LHS, the cumulative density function is divided into equal N partitions, and then a random number is sampled from one partition. In this way, LHS ensures that the entire range of input is covered.

The simplest method to map input with output is to create a scatter plot with an

input on the x-axis and an output on the y-axis. When the effect of one input on one output is measured, the method is called “one factor at a time” (OFAT). This approach is impractical when there are many parameters in the model because it requires the generation and evaluation of many plots. Therefore, regression and correlation methods have been applied to estimate qualitatively global sensitivity. Perhaps the most widely used tool is the partial rank correlation coefficient analysis (PRCC) where a partial rank correlation is calculated for the model inputs and outputs [88, 89].

5.2 Bifurcation analysis

In biological systems, values, among others, of protein synthesis rate or protein degradation rate are not constant but vary depending on for example the environment. Thus, to create a mathematical model of the biological system, it is important to study qualitatively model behavior when the values of the parameters vary several fold times.

Bifurcation analysis is a mathematical tool that is used to study the boundaries between regions in a wide parameter space where the qualitative behavior of a system varies drastically [90]. Therefore, a bifurcation analysis is performed to analyze a qualitative change in system behavior as a result of variation in a parameter (codim 1) or parameter values (codim >1).

Bifurcation theory has three practical applications. The most important one is in investigation boundaries between several types of dynamics of a biological system, such as a specific signaling pathway. It allows describing the behavior of the signaling pathway which behaves differently depending on environmental factors [83]. The second practical application is the adjustment of parameter values to obtain the desired system dynamics [91]. It is known as inverse bifurcation analysis. The last practical use of bifurcation analysis is to find the exact bifurcation point which is difficult to find experimentally [92]. One example of this application could be finding bifurcation points of cell cycles, which define the transitions between different cell cycle phases [93].

The most commonly observed bifurcations in biology are saddle-node and Hopf. The saddle-node bifurcation is also known as the fold bifurcation, and it is observed when two fixed points (the first is the saddle and the second is the node) collide and annihilate each other. In biology, this bifurcation is observed when the biological system works like a bi-stable switch. The most popular switch is the so-called toggle switch, which is frequently found in gene regulation [90]. Hopf bifurcation, on the other hand, is observed when a steady state solution becomes a periodic

solution as a result of change in the parameters values. Thus, Hopf bifurcation occurs when oscillations appear in the biological system.

6 Aims of the study

The main goal of this thesis is to develop mathematical models of resistance to treatment in solid tumors and apply them to suggest novel strategies to revert therapy resistance. The research aim can be divided into the following steps:

1. Develop a mathematical framework based on bifurcation theory and siRNA control to investigate how to restore proper functioning of the p53 pathway
2. Develop a stochastic mathematical model of innate resistance to platinum-based chemotherapy using longitudinal clinical data
3. Develop a mathematical framework to simulate a cohort of HGSOC patients
4. Develop a model of targeted therapy for HGSOC and simulate clinical trials

7 Materials, Methods, and Models

This thesis uses clinical data from advanced HGSOC patients and integrates them with mathematical modeling. An approximation of the stochastic simulation algorithm and numerical methods for solving ordinary differential equations (ODEs) were applied to achieve the model simulations. KM, SA, and bifurcation analyses were used to analyze the models. Table 1 presents the main methods used in this thesis.

Name	Category	Used in publication
Clinical data from HGSOC treated in TUH	data	II, III
TCGA clinical data from HGSOC patients	data	II, III
Branching process model	method	II, III
p53 signaling pathway model	method	I
Stochastic simulation algorithm	method	II, III
Kaplan–Meier analysis	method	II, III
Sensitivity analysis	method	II, III
Bifurcation analysis	method	I

Table 1: Summary of methods.

7.1 Clinical data

In this thesis, clinical data from patients with advanced HGSOC were collected to calibrate and validate the model. Firstly, the data from Turku University Hospital (TUH) were applied to calibrate the mathematical model (calibration cohort), and the data from TCGA were used as a validation cohort. Table 2 summarizes the patient characteristics.

The clinical data used in this thesis include the treatment schedule, response to primary treatment, progression data, and information about the tumor at the time of diagnosis, such as tumor stage and patient age. The key clinical parameter extracted from the clinical data is the platinum-free interval (PFI), which is measured as the time interval from the last date of platinum-based chemotherapy to relapse. PFIs were applied in the simulation framework to reproduce a real patient's response to therapy.

The calibration cohort includes data collected from HGSOC patients treated at TUH between 2009 and 2016. All of the patients were diagnosed as inoperable at the time of diagnosis and were, thus, treated using the NACT approach. That is, the patients were referred to the median of three cycles of NACT. The patients that

responded to NACT underwent interval debulking surgery, and patients that did not respond to NACT were referred to alternative or palliative treatment.

In addition, for the 26 HGSOC patients in the calibration cohort, ^{18}F–fluorodeoxyglucose positron emission tomography/computed tomography (^{18}F–FDG PET/CT) was performed before diagnostic laparoscopy and after median of the three NACT cycles [96]. Next, the metabolic tumor volume (MTV) was extracted from the ^{18}F–FDG PET/CT scans as a measure of tumor burden and converted from tumor volume to the number of cancer cells [97]. The data were applied to calculate the initial response to platinum-based chemotherapy in advanced HGSOC patients.

The validation cohort included data from the Cancer Genome Atlas (TCGA) where clinical data for 489 serous ovarian carcinoma patients are available. The patients were selected based on the following criteria: i) grade >1, ii) stage IIIb-IV, iii) patient underwent surgery, and iv) patient was treated with a platinum-taxane combination or platinum alone. After applying these selection criteria, a validation cohort of 170 HGSOC patients was created.

Characteristic	Calibration (n = 62)	TCGA (n = 170)
Age at diagnosis (years)	66	59
Tumor stage (FIGO 2009)		
IIIB	1	9
IIIC	37	134
IV	24	27
Residual tumor after DS		
0	14	26
1 to 10mm	27	87
>10mm	4	57
NA	16	0
Primary chemotherapy regimens		
Platinum	9	7
Platinum – Taxane	53	163
Primary therapy outcome		
Complete response	28	115
Partial response	13	25
Stable disease	0	8
Progressive disease	20	9
NA	1	13
Platinum-free interval (months)	5	7
Progression-free survival (months)	10	13
Overall survival (months)	18	37

Table 2: Summary of clinical data applied in the thesis. The data are presented as median or a number of patients. (adapted from Publication II)

7.2 Branching process model

The simplest branching process model is the Galton-Watson (G-W) model, which is also known as a discrete-time, discrete-state branching process model [76]. The model assumes a homogeneous population of X individuals, such as living cells. At every time step, each individual produces offspring independently of each other with rate λ. The dynamics of the number of cells in each generation is given using the following recursion formula:

$$X_{n+1} = \sum_{j=1}^{X_n} \xi_j^{(n)}.$$

where $\{\xi_j^{(n)} : j = 1,2,\dots\}$ is a set of independent and identically distributed random variables being equal to the number of progeny of the i-th individual (cell) of the n-th generation. The idea behind the G-W model is that individuals reproduce asexually, independently, and with the same distribution of offspring. The simplicity of the G-W process makes it frequently applied tool when studying processes of proliferation in biology and is applicable whenever the hypothesis of non-overlapping generations is justified.

The model can be modified easily to continuous-time discrete-state model as follows. A single individual (ancestor) is born at $t = 0$ and lives for time τ which is exponentially distributed with parameter λ. At the moment of death, the individual produces offspring according to the probability distribution with probability generating function $f(s)$. Next, each of the individuals in the next generation, behaves independently of each other, in the same way as the initial individual. It lives for a time interval equal to τ and produces a random number of offspring. Figure 6 presents four examples of simulations using the modified G-W model which is essentially identical to age-depended branching process model presented in chapter four in monograph [76].

Population growth can be modeled in continuous time also with a birth-death model. In that model, individuals produce offspring with the rate b throughout their lifetime, instead of reproduction only at the moment of death.Individuals die with the rate d, so that their life time is again exponentially distributed. The birth rate b can also be interpreted as the cell division rate when modeling the growth of cell populations. In that case the birth-death model can be interpreted as a continuous-time branching process model, in which life time is exponentially distributed with parameter $b+d$, and at the moment of death, an individual produces two offspring with probability $\frac{b}{b+d}$ and zero offspring with probability $\frac{d}{b+d}$. The transition probabilities for a simple birth-death process define the probability of a birth or death in a short period,

Δt, as follows: $p_{ij}(\Delta t) = \begin{cases} bi\Delta t, & \text{when } j = i+1 \\ di\Delta t, & \text{if } j = i-1 \\ 1-(b+d)i\Delta t & \text{if } j = i \\ 0, & \text{otherwise} \end{cases}$

The time increment Δt is chosen so that it is short with respect to the expected cell life-time which equals $1/\lambda$.

The model can also be expanded to a multiple-type individual case where we assume that at time of division, an individual has probability $b \cdot u$ to divide to a new type, where u is transition rate. The thesis focuses on the multiple–type continuous-time branching process where each cell type (subclone) has accumulated a different number of treatment resistance mechanisms.

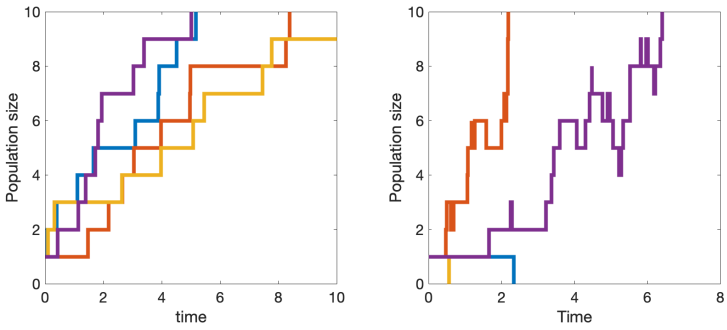

Figure 6: Exemplar four simulations of pure birth branching process model (left) and birth–death branching process (right). Each line shows one simulation starting from a single cell.

7.3 P53 signaling pathway model

P53 is the most crucial protein dysregulated in cancer. It is known as "the guardian of the genome" [94] because it is activated when DNA damage is detected, and its role is to stop the cell cycle and start the DNA repair program, and if it fails, to initiate apoptosis. Protein p53 is deactivated in half of the tumor types, and the p53 signaling pathway is the most frequently dysregulated pathway in cancer besides the MAPK pathway [95, 96]. Moreover, a mutation in p53 is connected to resistance to chemotherapeutic agents, such as cisplatin and doxorubicin [97, 98].

Figure 7 presents a schematic of a model applied in this thesis, Equations 1–4 describe the model, which is given in the form of the system of ordinary differential equations, and Table 3 lists the model parameters. This toy model of p53|Mdm2|PTEN system is based on two publications [99, 100]. The first shows

the appearance of oscillations in the system as a result of DNA damage, and the second publication describes the bi-stability of the p53 signaling pathway thanks to the positive feedback loop.

$$\frac{dp53}{dt} = p_1 - d_1\, p53(Mdm2_n)^2 \tag{1}$$

$$\frac{dMdm2_{cyt}}{dt} = p_2 \frac{(p53)^4}{(p53)^4 + (k_2)^4} - k_1 \frac{(k_3)^2}{(k_3)^2 + (PTEN)^2} Mdm2_{cyt} - d_2\, Mdm2_{cyt} \tag{2}$$

$$\frac{dMdm2_n}{dt} = k_1 \frac{(k_3)^2}{(k_3)^2 + (PTEN)^2} Mdm2_{cyt} - d_2\, Mdm2_n \tag{3}$$

$$\frac{dPTEN}{dt} = p_3 \frac{(p53)^4}{(p53)^4 + (k_2)^4} PTEN_{switch} - d_3 PTEN \tag{4}$$

In the model, p53 is produced spontaneously, and its level is regulated by the rate of his degradation controlled by Mdm2. The level of p53 is governed by positive and negative feedback loops. P53 actives cytoplasmic Mdm2 ($Mdm2_{cyt}$) and then Mdm2 is transported to the nucleus ($Mdm2_n$). Finally, Mdm2 degrades p53. It is a negative feedback loop inhibiting the possibility of a high level of p53. P53 also activates PTEN which inhibits transport of Mdm2 to the nucleus. It is a positive feedback loop which by inhibition of transport of Mdm2 to the nucleus, allows the increase of the level of p53.

Next, a more detailed model of the p53 signaling pathway was modified by the removal of system control by Nutlin, and the inclusion of irradiation (IR) and siRNA control. A schematic of the model is presented in Figure 1 of Publication I. The equations for the model are listed in the Supplementary Materials of Publication I.

7.4 Stochastic simulation algorithm

There are two main methods to solve mathematical models of biological systems: deterministic and stochastic ones depending on how the model is formulated. The deterministic methods include numerical algorithms to solve, e.g., the system of ODE whereas stochastic ones include methods to simulate biological systems by taking into account its heterogeneity.

Here, a method called the stochastic simulation algorithm (SSA) will be described as it is the most frequently applied method to simulate biological systems by taking into account stochasticity [101]. The most popular SSA method is called the Gillespie algorithm where the rate of each reaction is Poisson-distributed.

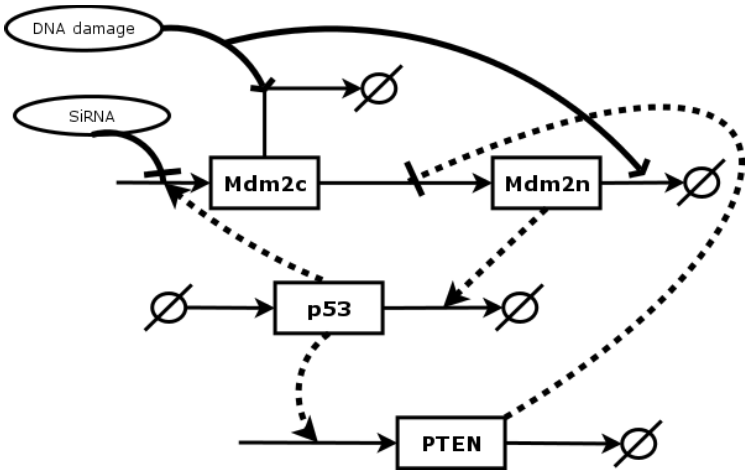

Figure 7: Schematic of the toy model of the p53 signaling pathway described in Equations 1–4. A solid line shows a transition from one type of molecule to another, and a dotted line represents activation. The arrow that ends with a vertical line represents inhibition.

In this thesis, the SSA was applied to simulate the dynamics of heterogeneous tumor mass, where many subclones are observed. As the appearance of a new subclone in the model simulation is a stochastic process, and the probability of a new mutation (and the emergence of a new subclone) is several folds smaller than the probability of faithful division, the SSA is the best method to simulate the evolution of drug resistance. Moreover, this algorithm allows us to simulate a heterogeneous population of patients.

Figure 8 presents a schematic of so-called direct method SSA, which works by answering two questions at each step of a simulation:

1. When will the next event occur?
2. Which event will happen next?

The Gillespie algorithm is easy to implement on a computer. First, we need to provide the population size for each species as the initial data. Next, we need to set all the possible interactions in the system by giving the event rate constant and a so-called transition matrix. Then, the propensity of each event is calculated according to the formula:

$$a_\mu = h_\mu \cdot C_\mu,$$

where h_μ is the number of all possible substrate combinations, and c_μ is the event rate constant. The next step is to generate two random numbers from uniform probability distribution between 0 and 1 that calculate the time of the next event and to determine which event will happen according to the formulas shown in Figure 9.

Symbol	Value	Description
p_1	$8.8\left[\frac{1}{s}\right]$	spontaneous production of p53
p_2	$440\left[\frac{1}{s}\right]$	Mdm2_{cyt} production rate
p_3	$100\left[\frac{1}{s}\right]$	PTEN production rate
d_1	$1.375 \cdot 10^{-14}\left[\frac{1}{s}\right]$	p53 degradation
d_2	$1.375 \cdot 10^{-5}\left[\frac{1}{s}\right]$	Mdm2_{cyt} degradation rate
d_3	$3 \cdot 10^{-5}\left[\frac{1}{s}\right]$	PTEN degradation rate
k_1	$1.925 \cdot 10^{-4}\left[\frac{1}{s}\right]$	transport rate of Mdm2_{cyt} to nucleus
k_2	10^5	inhibition constant for transport of Mdm2_{cyt} to nucleus
k_3	$1.5 \cdot 10^5$	activation constant for PTEN
DNA_{damage}	$0-9\ [a.u.]$	level of DNA damage
$PTEN_{switch}$	1	strength of positive feedback loop
$SiRNA_{dose}$	$0-1\ [a.u.]$	level of siRNA

Table 3: List of mathematical model parameters of mechanistic p53 signaling pathway model presented in Figure 7 .

Finally, the system is updated. The process continues until no reaction can happen or until the given simulation time.

7.5 Kaplan-Meier survival analysis

The Kaplan–Meier estimator is a statistical method that measures the survival probability over time by taking into account incomplete data [102]. In medicine, K-M analysis can be applied for example to estimate the fraction of patients who survive at a given time after treatment. It is the most widely used method for comparing two different arms in clinical trials. This thesis uses the K-M analysis to calibrate the stochastic model of innate drug resistance by taking into account real-life responses.

The Kaplan-Meier survival plot is defined as the probability function of surviving during a given period. Three assumptions are used in this analysis: The first is that patients who are censored have the same survival prospects as those who continue

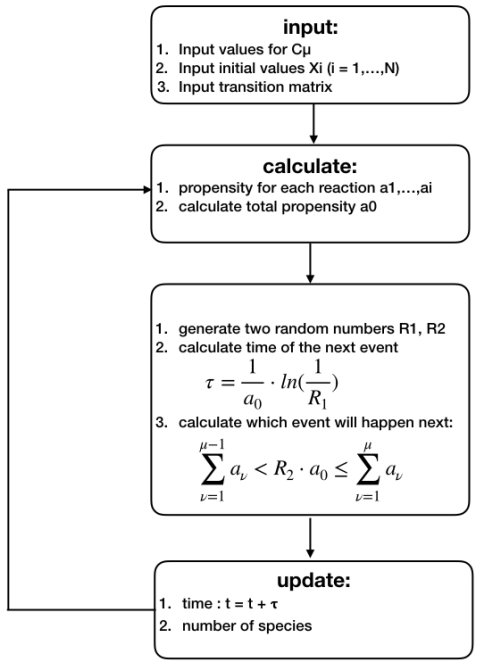

Figure 8: Schematic of stochastic simulation algorithm.

to be followed. In the second assumption, the survival probabilities are equal for patients who are recruited to the study at earlier or later phases. Third, it is assumed that the event happens at the exact time specified. In reality, an event, such as tumor recurrence, would not occur precisely at the time of the medical examination but between two follow-up appointments [103].

Formally, the Kaplan–Meier analysis is performed by calculating the survival probability at a given time using the following formula:

$$S_t = \frac{\text{number of subjects living at start} - \text{number of subjects died}}{\text{number of subjects living at start}}.$$

S_t is calculated as the number of surviving patients, divided by the number of patients at risk at a given time. Patients who are marked as "censored" because, for example, they dropped out, are not counted as "at risk." Therefore, censored patients are not counted in the denominator in the S_t equation. The total survival probability is calculated by multiplying all the probabilities at all time intervals that precede that time.

8 Results

This thesis uses the integrative mathematical oncology approach to investigate resistance to radiotherapy. Using a model of p53 signaling and siRNA control, we suggest a method to revert radio-resistance in cancer cells with damaged signaling pathways, which are responsible for apoptosis. Next, we develop a model of platinum resistance in advanced HGSOC and integrate it with longitudinal clinical data. The model is also used to find a novel drug combination for patients with advanced HGSOC using clinical trial simulations. Table 4 presents a summary of the results.

Name	Category	Used in publication
Application of bifurcation analysis and siRNA to radioresensitization	method	I
Stochastic model of innate platinum resistance in HGSOC	model	II, III
Virtual HGSOC patient cohort simulation approach	method	II, III
Integration of clinical data into mathematical model	method	II
Virtual clinical trials simulations in HGSOC	tool	III
Mathematical modeling targeted therapy in HGSOC	method	III

Table 4: Summary of results.

8.1 Radiosensitization using siRNA and bifurcation theory

Many types of p53 signaling dysregulations have been observed in cancer cells, whose repair could be vital in designing cancer treatment [104, 105]. This section investigates two types of p53 pathway damage: i) overexpression of p53 inhibitor, Mdm2, which is observed in 40% of cancer types such as osteosarcoma [106], and ii) silencing the PTEN protein that is observed for example in breast cancer [107]. PTEN is an inhibitor of the AKT pathway that is responsible for cell proliferation. The absence of this protein leads to uncontrolled cell growth. In the proposed model with system of ODE 1–4, the first p53 dysregulation is implemented by increasing production rate of Mdm2 ($p_{2\,new} = 8 \cdot p_2$) whereas the second one by setting $PTEN_{switch}$ to zero.

The main goal of performing a bifurcation analysis on a toy model of the p53 pathway is to investigate how disruption in the signaling pathway can change its

dynamics. This type of analysis has two applications in cancer research: i) to find a biomarker for a given type of cancer, and ii) to discover novel drug targets that restore proper functioning to the p53 signaling pathway. This thesis focuses on the second application and suggests siRNA as a means to control the dynamics of the p53 pathway.

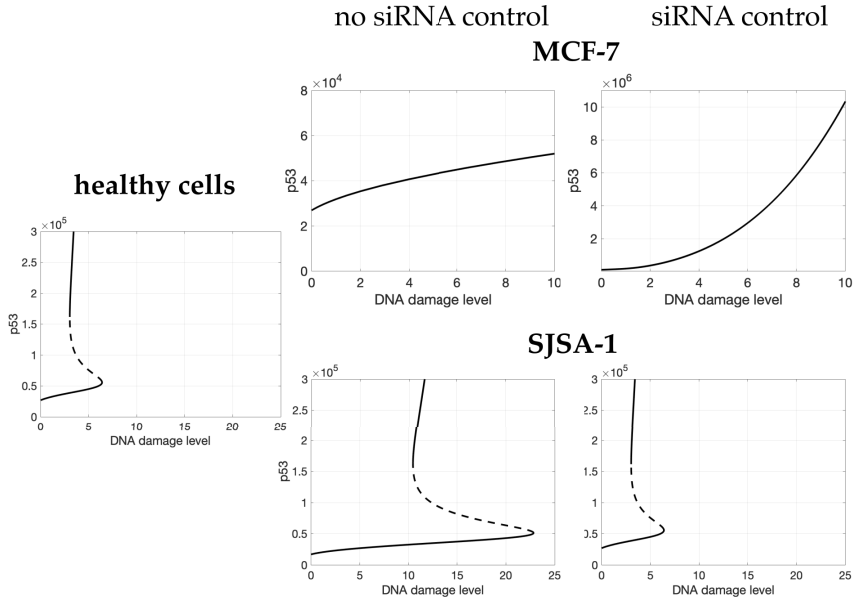

Figure 9: Bifurcation diagrams for healthy cells, MCF–7 cells (breast cancer), and SJSA–1 cells (osteosarcoma). Two bifurcation plots are shown for cells with damaged positive and negative feedback loops (MCF–7 and SJSA–1): the first considers a case without siRNA (left plot) and the second considers a case with siRNA (right plot). The solid and dotted lines represent stable and unstable equilibrium points, respectively.

Figure 9 presents the bifurcation plots for healthy, MCF–7, and SJSA–1 cells. The level of DNA damage was chosen as the bifurcation parameter. In healthy cells, the p53 signaling pathway behaves like a bistable switch. That is, low DNA damage activates the DNA repair pathway through a transient increase in the p53 level, which goes back down after the DNA is repaired. Intermediate DNA damage leads to bistability. That is, the cell can activate the DNA damage process, and the level of p53 goes back down or activates apoptosis by increasing the p53 level. Finally, a high level of DNA damage leads to a high level of p53 and activation of programmed cell death. In MCF-7 cells, we observe a drastic change in the dynamics of the p53 pathway. In this case, a system is monostable for a wide range of DNA damage with a low level of p53. Therefore, the disruption of the positive feedback loop makes it impossible for the cells to activate apoptosis. In SJSA-1

cells, we observe a shift in the bifurcation diagram to the right. As a result, p53 is activated in cells with a damaged negative feedback loop on a much higher level, which requires a higher dose of radiation.

Next, a bifurcation analysis was performed in a case where siRNA was included in the system to control the p53 pathway dynamics. As shown in Figure 9, the optimal level of extortion by siRNA for a high level of DNA damage leads to restoration of proper p53 dynamics in both types of cancer cells (MCF-7 and SJSA-1). Therefore, in $DNA_{damage} = 9$ the phase portraits for both types of cells are identical to those of healthy cells. Also, for SJSA-1 cells, the optimal level of siRNA leads to complete restoration of proper dynamics and results in the same bifurcation plot as healthy cells.

Finally, the results were confirmed using a detailed model of the p53 pathway, which includes two types of extorsions: Mdm2 siRNA and PTEN siRNA. The bifurcation analysis and p53 dynamics are in agreement with the results of the toy model. Furthermore, the mathematical modeling framework, which was based on the bifurcation theory, was extended to study the silencing of PTEN, using siRNA to immunize healthy cells against radiotherapy.

8.2 Mathematical model of innate resistance to platinum-taxane chemotherapy

Resistance to platinum-based drugs in ovarian cancer is a complex, multifactorial, and dynamical process [108, 109]. It is complex because many signaling pathways, including the apoptosis pathway [110], are involved in platinum resistance. Platinum resistance is also multifactorial because several platinum resistance mechanisms are believed to accumulate in the tumor. Moreover, resistance to platinum-based drugs is a dynamical process because most patients respond initially to platinum-based chemotherapy but relapse after a median of six months. We have developed a model of innate platinum resistance by taking these three properties of platinum resistance into account.

Figure 10 presents a schematic of a platinum resistance mathematical model and Table 2 in Publication II lists the model parameters used in this thesis. Briefly, a multitype continues time branching process model where each type of cell can undergo one of three processes: i) division to the same type of cell (faithful division) with rate $b(1-u)$, ii) division of the cell with an additional platinum drug resistance mechanism (unfaithful division) with rate $b \cdot u$, and iii) death with a rate of d. The model assumes an infinite number of possible subclones. That is, a wild-type cell acquires one platinum drug resistance mechanism, which leads to a subclone called

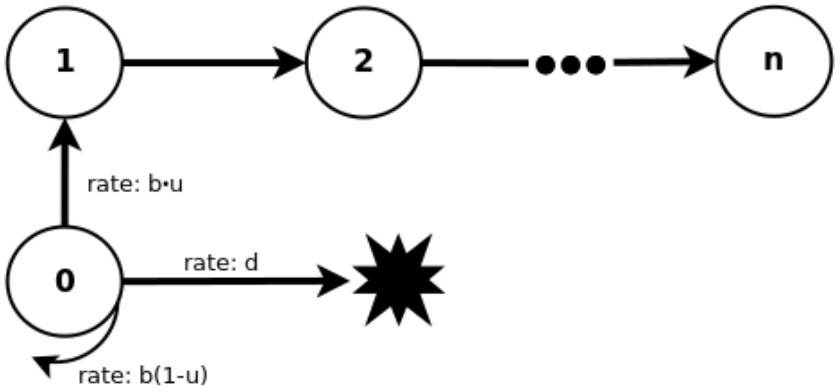

Figure 10: Schematic of the innate platinum resistance mathematical model, which assumes an infinite number of platinum resistance mechanisms.

"1" that can acquire an additional platinum drug resistance, leading to a subclone with two resistant platinum resistance mechanisms and so on. Therefore, the model assumes an infinite number of possible platinum resistance mechanisms.

In addition to modeling the growth of sensitive and resistant cells, two types of treatment interventions were modeled: platinum-based chemotherapy and debulking surgery. Chemotherapy is included in the model using the cell log-kill hypothesis, which increases the death rate in proportion to the birth rate. Debulking surgery is modeled by removing a fraction of β cells. All types of cells are removed with the same probability.

The major assumptions of the mathematical model are the following:

- Cells grow exponentially with a rate b.
- Cells with the acquired platinum resistance mechanism grow at the same rate as wild-type cells.
- All platinum drug resistance mechanisms accumulate sequentially with the same rate, u.
- During platinum-based chemotherapy, the rate of accumulation of platinum drug resistance is the same as in the absence of chemotherapy,
- Drug toxicity is not explicitly included in the model.

The mathematical modeling effort aimed to answer two clinically relevant questions:

1. What is the number of platinum drug resistance mechanisms in the tumor at the time of diagnosis?
2. How many platinum drug resistance mechanisms need to be targeted to achieve significant improvement in the patient's outcome?

The first question was answered using simulations of HGSOC patients until the diagnosis according to the standard of care in HGSOC. Next, a cell with the maximum number of platinum drug resistance mechanisms was extracted from the simulations. Finally, the average number of active platinum drug resistance mechanisms was calculated for a virtual cohort of 1,000 patients. Based on the model simulations, the advanced HGSOC patient accumulated five platinum drug resistance mechanisms (minimum two and maximum seven platinum resistance mechanisms) at the time of diagnosis.

The second clinical question was answered by simulating combination therapy. It was assumed that for each platinum drug resistance mechanism, there was a drug available with the same killing effect as the platinum-based chemotherapy. Therefore, a cohort of 1,000 virtual patients was created, and one to six drugs targeting platinum resistance were administered together with platinum. As we can see in Figure 4 in Publication II, using more than three drugs to target platinum drug resistance does not improve the platinum-free interval. Therefore, we concluded that it was sufficient to target the three major mechanisms, even though five platinum drug resistance mechanisms were present in the HGSOC patients at the time of diagnosis.

8.3 Standard of care in advanced HGSOC simulator

This thesis develops a computer simulator of SOC in advanced HGSOC, which is presented schematically in Figure 11. The simulator includes three phases: pre-treatment, treatment, and post-treatment. The goal is to create a simulator that captures real-life responses to HGSOC *in silico*.

For each virtual HGSOC patient, two parameters are sampled from lognormal distribution before the simulation begins: i) tumor burden at diagnosis (M) and ii) chemotherapy-induced death rate ($d_{chemotherapy}$). Next, the pre-treatment phase starts from a single wild-type cell, and the tumor grows according to the exponential growth model in the absence of treatment interventions. The pre-treatment phase ends when the total number of tumor cells is equal to M.

The treatment phase includes two types of interventions: i) platinum-based chemotherapy and ii) debulking surgery according to NCCN [33]. Since clinical data from patients in the calibration cohort are from patients who cannot be operated at the time of diagnosis, the treatment phase is simulated as follows. First, a virtual HGSOC patient is treated with three cycles of neoadjuvant platinum-based chemotherapy. Next, debulking surgery is performed by removing at a one-time point fraction of β cancer cells. Finally, three cycles of adjuvant chemotherapy are administered.

The last phase of simulation is called post-treatment. In this phase, the virtual HGSOC patient has a small invisible tumor and no symptoms. This phase is simulated as the pre-treatment phase where the tumor grows without interventions. The phase ends when the tumor reaches $M_{relapse} = 10^9$ cells, which is the smallest detectable tumor size.

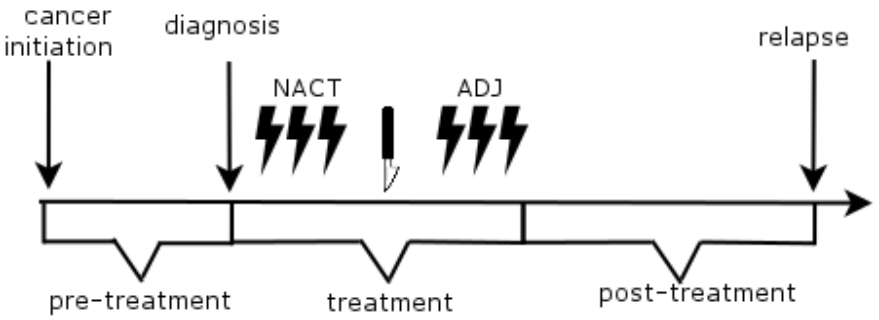

Figure 11: Schematic of standard–of–care simulations. The model simulation starts from a single wild-type cell until the diagnosis – pre-treatment phase. Next phase is a treatment consisting of platinum-taxane chemotherapy and debulking surgery. Finally, the post-treatment phase is simulated until the first relapse, and PFI is calculated.

8.4 Integration of clinical data into mathematical model

The data from the calibration cohort were applied to estimate the model parameters. In brief, MTV data from PET/CT scans at the time of diagnosis and after three cycles of NACT were used together with the response data measured as the platinum-free interval (PFI). Since this thesis focuses on primary treatment and the first relapse, only the first PFI (the time interval between the end of primary treatment and the first relapse) was measured. Figure 12 shows how the clinical data were integrated into the model.

The PET/CT data at the time of diagnosis were applied to compute the probability distribution of clinical diagnosis as a function of tumor burden (to estimate parameter M). The data were fitted to the following probability distribution function: normal, exponential, Weibull, log-normal, logistic, and log-logistic. Next, the Bayesian Information Criterion (BIC) was calculated for each distribution to measure the goodness of fit (GOF) of the data to the probability distribution. The best fit was obtained for log-normal distribution and was applied accordingly.

Furthermore, PET/CT data were applied at two-time points (at the time of diagnosis and after NACT) to calculate the killing effect of platinum-based chemotherapy. For each patient, this parameter was fitted using the bisection method to find the

minimum value for the following objective function:

$$J = \hat{M_{NACT}} - M_{NACT} = \sum_{i=1}^{n} (t_{NACT}) - M_{NACT},$$

where M_{NACT} and $\hat{M_{NACT}}$ are the tumor burden after NACT and prediction based on the model simulations, respectively. Based on these results, the killing effect of platinum chemotherapy for each patient in the calibration cohort was estimated. Next, the killing effect values were fitted to the probability distributions where the best GOF was obtained for log-normal one.

Next, the PFI values were applied to find a value for the transition rate u. Firstly, the K-M plot was created for the PFI data from the calibration cohort. As explained in the previous section, SOC simulations were performed to generate a cohort of 1,000 virtual HGSOC patients. From these simulations, the PFI was extracted, and the K-M plot was created in the same way as the PFIs from the calibration cohort. Finally, the two plots were compared using the root mean squared error (RMSE). The model was simulated for a wide range of u and compared to data using RMSE. The value of parameter u with the smallest RMSE was chosen.

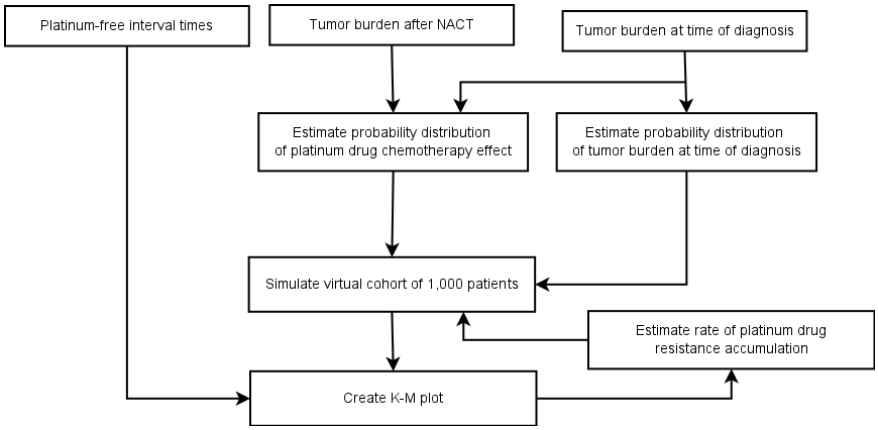

Figure 12: Integration of longitudinal clinical data into the mathematical model of platinum drug resistance. The clinical data were applied to find the value of the following parameters in the model: tumor burden at diagnosis ($M_{diagnosis}$), transition rate (u), and effect of platinum-taxane chemotherapy ($d_{chemotherapy}$).

8.5 Mathematical modeling of targeted therapy in HGSOC

The next goal of the modeling effort was to suggest a combination treatment to overcome platinum drug resistance. The results from genomic studies and other mathematical modeling efforts show that ovarian cancer is already resistant

to platinum at the time of diagnosis [111, 112]. Therefore, a combination of platinum-based chemotherapy and a drug that targets the given platinum drug resistance mechanism is suggested. Figure 13 presents the schematic model of targeted therapy. In brief, three drugs were included: trientine, Wee1 inhibitor, and birinapant, which are effective in treating pre-, on–, and post–target platinum drug resistance, respectively. The drugs that were chosen via the literature review have shown promise when combined with platinum-based chemotherapy and are currently in the late stages of clinical trials.

The first drug included in the model is trientine, which targets platinum drug resistance caused by reduced platinum drug uptake (pre-target resistance). It is known that the active transport of a platinum drug into a cell is mediated through copper transporter receptor 1 (CTR1). Trientine enhances Ctr-mediated platinum transport to the cell. The drug is included in the model by increasing the killing effect of the platinum drug in partially-resistant cells.

The second drug included in the model is Wee1 inhibitor, which targets on-target platinum drug resistance. The Wee1 inhibitor inhibits Wee1 kinase, which is responsible for the modulation of DNA damage response (DDR). The predominant mechanism of action in Wee1 inhibitors is the failure of the G2–M checkpoint, which occurs due to inappropriate CDK1/CCNB1 activation. Wee1 inhibition also generates replication-dependent DNA damage in cells. Therefore, the Wee1 inhibitor re-sensitizes a cell to platinum-based chemotherapy. In the model, the drug is included through a backward transition of a cell from fully-resistant to partially-resistant and from partially-resistant to sensitive.

The third drug included in the model is birinapant, which is known as an inhibitor of apoptosis (IAP). IAP is a crucial regulator of programmed cell death and hence targeting post-target platinum drug resistance. The drug is included by adding additional death to the model called apoptosis. In this process, a cell with a post-target platinum drug resistance mechanism remains active but dies in the presence of birinapant, creating an additional apoptotic death rate.

8.6 Virtual clinical trials simulations in HGSOC

In this thesis, virtual clinical trials simulations (VCTS) approach was applied to answer two questions i) what is the effectiveness of platinum-based chemotherapy combined with targeted therapy to overcome platinum drug resistance? And ii) what is the benefit of targeting dominant platinum drug resistance mechanisms using molecular biomarkers? Thus, two types of VCTS are performed: randomized controlled trial simulations RCTS and molecularly-stratified controlled trials simulations MSCTS.

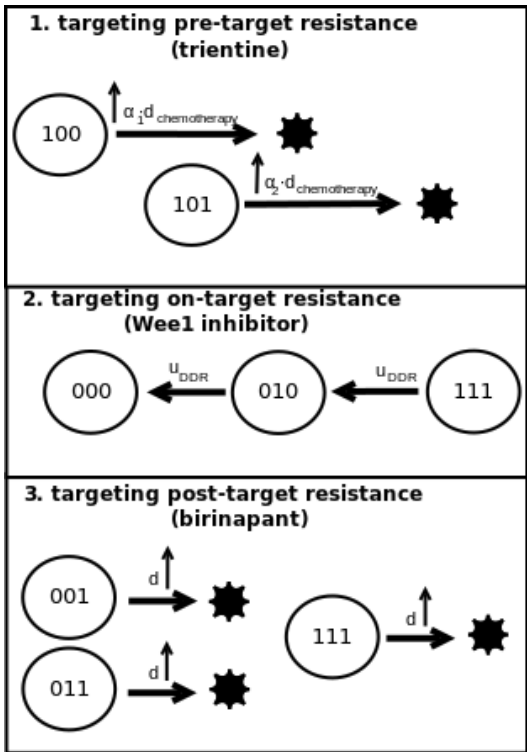

Figure 13: Mathematical modeling of targeted therapy in HGSOC. we have included three drugs trientine, Wee1 inhibitor, and birinapant, which target pre-, on- and post-target platinum resistance, respectively.

Firstly, simulations have been performed for a combination of trientine, Wee1 inhibitor or birinapant with platinum-based chemotherapy. The best one–drug combination was obtained for Wee1 inhibitor which triple PFI in comparison to platinum-based chemotherapy alone. The worst combination is with birinapant which gives only three months improvement in PFI. We can conclude that a drug which re-sensitize cells to platinum-based chemotherapy leads to a better outcome than a drug such as trientine which is directly killing resistant cells.

Next, two–drugs combinations were tested with platinum-based chemotherapy and obtained that Wee1 inhibitor combined with birinapant gives the best outcome as the PFI is equal to 30 months. The worst combination was for birinapant, and trientine with PFI equals to 17 months. Finally, a combination of three drugs (trientine, Wee1 inhibitor, and birinapant) showed a massive reduction of tumor burden and PFI equal to 34 months.

We have also performed clinical trials where biomarkers are applied to stratify

patients into different treatment groups. Patients were stratified according to their dominant platinum resistance mechanism. As Table 2 in Publication III shows, the benefit of choosing patients positive to trientine and birinapant has four and six months improvement in comparison to negative one, respectively. For Wee1, however, no significant rise is observed. Based on MSCTS, the benefit of patient stratification depends on drug efficacy and tumor composition.

9 Discussion

The development of novel mathematical tools, together with advancements in biological experimentation tools, has allowed for the emergence of a new field called integrative mathematical oncology. This new field of cancer research focuses on understanding cancer from a mathematical perspective. I used the IMO approach, in this thesis, to study resistance to therapy in a solid tumor.

Specifically, this thesis focuses on understanding the resistance to radio- and chemotherapy in solid tumors on the molecular and cellular levels using mathematical tools. Since evading cell death is one of the hallmarks of cancer and a cause of therapy resistance, we focus on the p53 signaling pathway that regulates apoptosis. Indeed, targeting this pathway could revert resistance to therapy in patients with ovarian cancer, as well as other types of cancer [113, 114]. Next, we concentrated on understanding resistance to SOC in patients with advanced HGSOC and suggested novel combinatorial treatments for this aggressive type of cancer. In this case, resistance to treatment was modeled on the cellular level.

In Publication I, we developed a mathematical framework that was based on bifurcation theory and siRNA control to suggest a method to re-sensitize cancer cells with two types of disruptions in the p53 signaling pathway to radiotherapy. Since the p53 signaling pathway is one of the most commonly disrupted in solid tumors, we created a kinetic model of this pathway for solid tumors. Next, an inverse bifurcation analysis was performed to find the values of the parameters in the dysregulated p53 signaling pathway which could restore its proper dynamics. An analysis conducted on a toy model suggested silencing Mdm2, which is an inhibitor of p53. Next, the model was validated using a more complex model of the p53 signaling pathway.

The p53 signaling pathway is a very complex pathway with many negative and positive feedback loops. Therefore, the creation of a more complex p53 signaling pathway model that incorporates other important feedback loops would advance this research. For example, it is known that the p53 signaling pathway has cross-talks with the NFkB and ATM pathways. Testing this method on another commonly dysregulated pathway, such as the MAPK pathway, which controls cell proliferation, would be another way to advance this research.

In Publication II, we created a mathematical model of platinum resistance in advanced high-grade serous ovarian cancer. In a previous modeling effort, platinum resistance was assumed to be unifactorial; however, platinum resistance is in fact multifactorial. Therefore, a stochastic model was built based on the branching process, taking into account the multifactorial nature of platinum resistance. The

model was applied to answer two vital clinical questions: How many platinum resistance mechanisms are present at the time of diagnosis? And How many drug resistance mechanisms need to be targeted to improve patient outcomes?

We applied longitudinal clinical data from advanced HGSOC patients to reproduce an initial and long-term response to platinum. The initial response was measured using PET/CT scans, which showed that the median three cycles of NACT reduced the tumor by 80%. The long-term response, however, was measured using a platinum-free-interval with a median value of six months. Inter-patient heterogeneity was also reproduced by sampling two clinical parameters from a random probability distribution.

The platinum resistance model could be extended by modeling other treatment strategies in ovarian cancer. For instance, another approach in SOC for HGSOC patients is primary debulking surgery followed by adjuvant chemotherapy. Besides, the model presented in this thesis does not consider a combination of platinum chemotherapy and maintenance therapy with bevacizumab, which is being applied more frequently in clinics. Thus modeling bevacizumab treatment could advance this research.

In Publication III, we created a model of platinum resistance, which considered three platinum resistance mechanisms: pre-, on-, and post-target. Next, we combined it with a model of targeted therapy that includes three drugs: trientine, Wee1 inhibitor, and birinapant, which are effective at treating pre-, on-, and post-target resistance mechanisms, respectively. We also suggested a novel mathematical method to calculate the drug efficacy of a drug that is currently in the late stage of a clinical trial.

In Publication III, we applied a virtual clinical trial approach to estimate the benefits of targeted therapy in advanced HGSOC. We performed two types of VCTS: i) a randomized controlled trial (RCT) and ii) a molecularly stratified controlled trial (MSCT). The first trial estimated the effectiveness of targeted therapy in the non-stratified HGSOC patient cohort. Based on the VCTS, Wee1 inhibitor was identified as the most effective drug, which means that a drug that re-sensitizes cells to platinum provides the best outcome in terms of longer PFI. Next, we performed an MSCTS to investigate the benefits of targeting the dominant drug resistance mechanism. The simulations showed the benefits of patient stratification based on a dominant platinum resistance mechanism when using two out of three drugs. It indicates that targeting the dominant platinum resistance mechanism could prolong PFI.

The model of platinum resistance combined with a targeted therapy could be advanced, among others, by incorporating drug toxicity. The model presented in

this thesis assumes that drugs kill cancer cells but do not affect healthy cells. Even though a combination of platinum with one targeted drug shows acceptable toxicity, it might not be tolerated in a combination of two or three drugs. The model could also be extended by modeling the pharmacokinetics of the drug, which would allow for optimization of the drug dose.

In conclusion, the mathematical oncology approach was applied to understand the resistance to chemotherapy and radiotherapy in solid cancers on the molecular and cellular levels. We suggested a method to overcome radio-resistance in breast cancer and osteosarcoma by applying bifurcation theory and siRNA control. Next, we built a model of platinum resistance in HGSOC on the cellular level and modeled the evolution of various subclones with different levels of platinum resistance. Integrating the model with longitudinal clinical data allowed us to answer urgent clinical questions related to ovarian cancer. Finally, the VCTS approach was used to suggest novel drug combinations in HGSOC that could improve patient outcomes.

As a future development, IMO will continue to integrate longitudinal clinical and multi-omics molecular data with mathematical modeling to create a patient-specific model. Current mathematical models have not been applied successfully in the clinical setting since model parameters are estimated based on data from *in vitro* and *in vitro* experiments. Models that are based on clinical data have the advantage of being based on information that is directly extracted from patients. Next, the development of mathematical tools allowing integration of patient's data with mathematical modeling will continue. Lastly, advances in hybrid and multiscale mathematical modeling will allow modeling tumor on several scales simultaneously.

Acknowledgements

This work was carried out in the Systems Biology Laboratory at the Faculty of Medicine, the University of Helsinki during 2014-2018. This study was financially supported by Integrative Life Science Doctoral Graduate Program, Sigrid Juselius Foundation, Finnish Cancer Associations, and the European Union's Horizon 2020 Research and Innovation Programme.

First of all, I would like to express my gratitude to Prof Sampsa Hautaniemi who was supervising my doctoral project. I thank you for providing me sufficient research resources and your support. You always had time to discuss with me on various scientific topics what tremendously helped me to become an independent researcher. I especially thank for a long discussion about how to apply my models in the clinic because it helps me to become true mathematical oncologist.

I thank the members of my thesis committee, professor Tero Aittokallio and docent Ion Petre, for their support and advice during the annual meetings and between them.

I wish to thank the reviewers of my thesis, docent Kalle Parvinen and professor Andre Ribeiro, for their time and useful comments to my thesis work.

I am grateful to clinicians from University Turku Hospital: Prof Seija Grénman, Prof Olli Carpén, Johanna Hynninen, Sakari Hietanen, Jukka Kemppainen and Tuulia Vallius for providing me longitudinal clinical data and PET/CT scans data allowing me to parametrize mathematical models. With your input, my work is truly integrative mathematical oncology.

I would like to thanks Anniina Färkkilä for guidance in the clinical part of my project. Without your insightful feedback and suggestions, my work would be purely theoretical. Thank you for helping me to connect the results of my simulations with reality. It was indeed a pleasure to work with you!

I am also grateful to my mathematical collaborators: Krzysztof Puszyński and Prof Marek Kimmel. Krzysztof Puszyński who was supervising my master thesis, introduced me to an exciting field of mathematical oncology. Thank you for your guidance and support in the mathematical part of my thesis. I would also like to thank Prof. Marek Kimmel, whom I met during q–bio summer school, for fruitful collaboration and weekly discussion about biology and mathematics.

I thank all the past and current members in our lab. Special thanks go to Julia with whom I discuss on various topics related to science. I also thank Chiara and Rainer for reading and commenting on my thesis manuscript.

Lastly, my deepest gratitude to my parent and my brother for your support on my way to becoming scientists. You always encouraged me in my passion for mathematics and physics. I would like to thanks my friends: Andrew, Anna–Riina, Dominika, Kasia, Laura, Luis, Lissy, Nati, Maciej, Markku, Paulina, and Tea for encouragement and help in difficult time.

Emilia Kozłowska
Helsinki, 2019

References

Page(s)

[1] Anderson, A. R & Maini, P. K. (2018) Mathematical Oncology. *Bulletin of Mathematical Biology* **80**, 945–953.
1

[2] Byrne, H. M. (2010) Dissecting cancer through mathematics: from the cell to the animal model. *Nature Reviews Cancer* **10**.
1

[3] Deisboeck, T. S, Wang, Z, Macklin, P, & Cristini, V. (2011) Multiscale cancer modeling. *Annual review of biomedical engineering* **13**, 127–55.
1

[4] Neal, M. L & Kerckhoffs, R. (2009) Current progress in patient-specific modeling. *Briefings in Bioinformatics* **11**, 111–126.
1

[5] Anderson, A. R. A & Quaranta, V. (2008) Integrative mathematical oncology. *Nature Reviews Cancer* **8**, 227–234.
1

[6] Anderson, A. R. A & Maini, P. K. (2018) Mathematical Oncology. *Bulletin of Mathematical Biology* **80**, 945–953.
1

[7] Chauviere, A. H, Hatzikirou, H, Lowengrub, J. S, Frieboes, H. B, Thompson, A. M, & Cristini, V. (2010) Mathematical Oncology: How Are the Mathematical and Physical Sciences Contributing to the War on Breast Cancer? *Current breast cancer reports* **2**, 121–129.
1

[8] Nik-Zainal, S, Van Loo, P, Wedge, D. C, Alexandrov, L. B, Greenman, C. D, Lau, K. W, Raine, K, Jones, D, Marshall, J, Ramakrishna, M, Shlien, A, Cooke, S. L, Hinton, J, Menzies, A, Stebbings, L. A, Leroy, C, Jia, M, Rance, R, Mudie, L. J, Gamble, S. J, Stephens, P. J, McLaren, S, Tarpey, P. S, Papaemmanuil, E, Davies, H. R, Varela, I, McBride, D. J, Bignell, G. R, Leung, K, Butler, A. P, Teague, J. W, Martin, S, Jönsson, G, Mariani, O, Boyault, S, Miron, P, Fatima, A, Langerod, A, Aparicio, S. A, Tutt, A, Sieuwerts, A. M, Borg, Å, Thomas, G, Salomon, A. V, Richardson, A. L, Borresen-Dale, A. L, Futreal, P. A, Stratton, M. R, & Campbell, P. J. (2012) The life history of 21 breast cancers. *Cell* **149**, 994–1007.
1

[9] Komarova, N. L, Burger, J. A, & Wodarz, D. (2014) Evolution of ibrutinib resistance in chronic lymphocytic leukemia (CLL). *Proceedings of the National Academy of Sciences* **111**, 13906–13911.
1, 15

[10] Brown, P. O & Palmer, C. (2009) The preclinical natural history of serous ovarian cancer: Defining the target for early detection. *PLoS Medicine* **6**, e1000114.
1

[11] He, L, Wennerberg, K, Aittokallio, T, & Tang, J. (2015) *TIMMA-R: An R package for predicting synergistic multi-targeted drug combinations in cancer cell lines or patient-derived samples*. (Oxford University Press), Vol. 31, pp. 1866–1868.
1

[12] Rejniak, K. A & McCawley, L. J. (2010) Current trends in mathematical modeling of tumor–microenvironment interactions: a survey of tools and applications. *Experimental Biology and Medicine* **235**, 411–423. 1

[13] Stein, S, Zhao, R, Haeno, H, Vivanco, I, & Michor, F. (2018) Mathematical modeling identifies optimum lapatinib dosing schedules for the treatment of glioblastoma patients. *PLOS Computational Biology* **14**, e1005924. 1

[14] Benzekry, S, Tracz, A, Mastri, M, Corbelli, R, Barbolosi, D, & Ebos, J. M. (2016) Modeling spontaneous metastasis following surgery: An in vivo-in silico approach. *Cancer Research* **76**, 535–547. 1

[15] Gallasch, R, Efremova, M, Charoentong, P, Hackl, H, & Trajanoski, Z. (2013) Mathematical models for translational and clinical oncology. *Journal of clinical bioinformatics* **3**, 23. 2

[16] National Cancer Institute. (2018) Homeostasis. *NCI Dictionary of Cancer Terms*. 3

[17] Falco, M, Palma, G, Rea, D, De Biase, D, Scala, S, D'Aiuto, M, Facchini, G, Perdonà, S, Barbieri, A, & Arra, C. (2016) Tumour biomarkers: homeostasis as a novel prognostic indicator. *Open biology* **6**. 3

[18] Fouad, Y. A & Aanei, C. (2017) Revisiting the hallmarks of cancer. *American Journal of Cancer Research* **7**, 1016–1036. 3

[19] Meinhold-Heerlein, I, Fotopoulou, C, Harter, P, Kurzeder, C, Mustea, A, Wimberger, P, Hauptmann, S, & Sehouli, J. (2016) Erratum to: The new WHO classification of ovarian, fallopian tube, and primary peritoneal cancer and its clinical implications. 3

[20] Song, Q, Merajver, S. D, & Li, J. Z. (2015) Cancer classification in the genomic era: five contemporary problems. *Human genomics* **9**, 27. 3

[21] Weinberg, R. A. R. A. (2014) *The biology of cancer*. (Garland science), pp. 31—-69. 3

[22] National Cancer Institute. (2018) Solid tumor. *NCI Dictionary of Cancer Terms*. 3

[23] Bray, F, Ferlay, J, Soerjomataram, I, Siegel, R. L, Torre, L. A, & Jemal, A. (2018) Global cancer statistics 2018: GLOBOCAN estimates of incidence and mortality worldwide for 36 cancers in 185 countries. *CA: A Cancer Journal for Clinicians* **68**, 394–424. 3

[24] Buys, S. S, Partridge, E, Black, A, Johnson, C. C, Lamerato, L, Isaacs, C, Reding, D. J, Greenlee, R. T, Yokochi, L. A, Kessel, B, Crawford, E. D, Church, T. R, Andriole, G. L, Weissfeld, J. L, Fouad, M. N, Chia, D, O'Brien, B, Ragard, L. R, Clapp, J. D, Rathmell, J. M, Riley, T. L, Hartge, P, Pinsky, P. F, Zhu, C. S, Izmirlian, G, Kramer, B. S, Miller, A. B, Xu, J. L, Prorok, P. C, Gohagan, J. K, & Berg, C. D. (2011) Effect of screening on ovarian cancer mortality: The Prostate, Lung, Colorectal and Ovarian (PLCO) cancer screening randomized controlled trial. *JAMA - Journal of the American Medical Association* **305**, 2295–2302. 3

[25] Chen, V. W, Ruiz, B, Killeen, J. L, Coté, T. R, Wu, X. C, Correa, C. N, & Howe, H. L. (2003) Pathology and classification of ovarian tumors. *Cancer* **97**, 2631–2642. 3

[26] Desai, A. (2014) Epithelial ovarian cancer: An overview. *World Journal of Translational Medicine* **3**, 1.
3

[27] Bowtell, D. D, Böhm, S, Ahmed, A. A, Aspuria, P.-J, Bast, R. C, Beral, V, Berek, J. S, Birrer, M. J, Blagden, S, Bookman, M. A, Brenton, J. D, Chiappinelli, K. B, Martins, F. C, Coukos, G, Drapkin, R, Edmondson, R, Fotopoulou, C, Gabra, H, Galon, J, Gourley, C, Heong, V, Huntsman, D. G, Iwanicki, M, Karlan, B. Y, Kaye, A, Lengyel, E, Levine, D. A, Lu, K. H, McNeish, I. A, Menon, U, Narod, S. A, Nelson, B. H, Nephew, K. P, Pharoah, P, Powell, D. J, Ramos, P, Romero, I. L, Scott, C. L, Sood, A. K, Stronach, E. A, & Balkwill, F. R. (2015) Rethinking ovarian cancer II: reducing mortality from high-grade serous ovarian cancer. *Nature Reviews Cancer* **15**, 668–679.
3

[28] Kohn, E. C, Romano, S, & Lee, J.-M. (2013) Clinical implications of using molecular diagnostics for ovarian cancers. *Annals of Oncology* **24**, x22–x26.
4

[29] Bashashati, A, Ha, G, Tone, A, Ding, J, Prentice, L. M, Roth, A, Rosner, J, Shumansky, K, Kalloger, S, Senz, J, Yang, W, McConechy, M, Melnyk, N, Anglesio, M, Luk, M. T, Tse, K, Zeng, T, Moore, R, Zhao, Y, Marra, M. A, Gilks, B, Yip, S, Huntsman, D. G, McAlpine, J. N, & Shah, S. P. (2013) Distinct evolutionary trajectories of primary high-grade serous ovarian cancers revealed through spatial mutational profiling. *The Journal of Pathology* **231**, 21–34.
4

[30] Torre, L. A, Trabert, B, DeSantis, C. E, Miller, K. D, Samimi, G, Runowicz, C. D, Gaudet, M. M, Jemal, A, & Siegel, R. L. (2018) Ovarian cancer statistics, 2018. *CA: A Cancer Journal for Clinicians* **68**, 284–296.
4

[31] Bell, D, Berchuck, A, Birrer, M, Chien, J, Cramer, D. W, Dao, F, Dhir, R, DiSaia, P, Gabra, H, & Al., E. (2011) Integrated genomic analyses of ovarian carcinoma. *Nature* **474**, 609–615.
4

[32] Ledermann, J. A, Raja, F. A, Fotopoulou, C, Gonzalez-Martin, A, Colombo, N, Sessa, C, & ESMO Guidelines Working Group. (2013) Newly diagnosed and relapsed epithelial ovarian carcinoma: ESMO Clinical Practice Guidelines for diagnosis, treatment and follow-up. *Annals of oncology* **24 Suppl 6**, vi24–32.
4

[33] Armstrong, D. K. (2018) New Therapies for Ovarian Cancer. *Journal of the National Comprehensive Cancer Network* **16**, 632–635.
4, 34

[34] Montagnana, M, Danese, E, Ruzzenente, O, Bresciani, V, Nuzzo, T, Gelati, M, Salvagno, G. L, Franchi, M, Lippi, G, & Guidi, G. C. (2011) The ROMA (Risk of Ovarian Malignancy Algorithm) for estimating the risk of epithelial ovarian cancer in women presenting with pelvic mass: is it really useful? *Clinical Chemistry and Laboratory Medicine* **49**, 521–5.
4

[35] Polterauer, S, Vergote, I, Concin, N, Braicu, I, Chekerov, R, Mahner, S, Woelber, L, Cadron, I, Van Gorp, T, Zeillinger, R, Castillo-Tong, D. C, & Sehouli, J. (2012) Prognostic value of residual tumor size in patients with epithelial ovarian cancer FIGO stages IIA-IV: Analysis of the OVCAD data. *International Journal of Gynecological Cancer* **22**, 380–385.
4

[36] Hanahan, D & Weinberg, R. (2011) Hallmarks of Cancer: The Next Generation. *Cell* **144**, 646–674.
5

[37] Feitelson, M. A, Arzumanyan, A, Kulathinal, R. J, Blain, S. W, Holcombe, R. F, Mahajna, J, Marino, M, Martinez-Chantar, M. L, Nawroth, R, Sanchez-Garcia, I, Sharma, D, Saxena, N. K, Singh, N, Vlachostergios, P. J, Guo, S, Honoki, K, Fujii, H, Georgakilas, A. G, Bilsland, A, Amedei, A, Niccolai, E, Amin, A, Ashraf, S. S, Boosani, C. S, Guha, G, Ciriolo, M. R, Aquilano, K, Chen, S, Mohammed, S. I, Azmi, A. S, Bhakta, D, Halicka, D, Keith, W. N, & Nowsheen, S. (2015) Sustained proliferation in cancer: Mechanisms and novel therapeutic targets. *Seminars in Cancer Biology* **35**, S25–S54.
5

[38] Vineis, P, Schatzkin, A, & Potter, J. D. (2010) Models of carcinogenesis: An overview. *Carcinogenesis* **31**, 1703–1709.
5

[39] Nowell, P. C. (1976) The clonal evolution of tumor cell populations. *Science* **194**, 23–8.
5, 6

[40] Adams, J. M & Strasser, A. (2008) Is tumor growth sustained by rare cancer stem cells or dominant clones? *Cancer Research* **68**, 4018–4021.
5, 6

[41] Merlo, L. M, Pepper, J. W, Reid, B. J, & Maley, C. C. (2006) Cancer as an evolutionary and ecological process. *Nature Reviews Cancer* **6**, 924–935.
6

[42] Greaves, M & Maley, C. C. (2012) Clonal evolution in cancer. *Nature* **481**, 306–313.
6

[43] Maley, C. C, Aktipis, A, Graham, T. A, Sottoriva, A, Boddy, A. M, Janiszewska, M, Silva, A. S, Gerlinger, M, Yuan, Y, Pienta, K. J, Anderson, K. S, Gatenby, R, Swanton, C, Posada, D, Wu, C. I, Schiffman, J. D, Hwang, E. S, Polyak, K, Anderson, A. R, Brown, J. S, Greaves, M, & Shibata, D. (2017) Classifying the evolutionary and ecological features of neoplasms. *Nature Reviews Cancer* **17**, 605–619.
6

[44] Gatenby, R. A, Silva, A. S, Gillies, R. J, & Frieden, B. R. (2009) Adaptive therapy. *Cancer Research* **69**, 4894–4903.
7

[45] Bookman, M. A. (2016) Optimal primary therapy of ovarian cancer. *Annals of Oncology* **27**, i58–i62.
7

[46] Benjamin, D. J. (2014) The efficacy of surgical treatment of cancer - 20 years later. *Medical Hypotheses* **82**, 412–420.
7

[47] Schorge, J. O, McCann, C, & Del Carmen, M. G. (2010) Surgical debulking of ovarian cancer: what difference does it make? *Reviews in obstetrics & gynecology* **3**, 111–7.
7

[48] Matsen, C. B & Neumayer, L. A. (2013) Breast Cancer. *JAMA Surgery* **148**, 971.
7

[49] Bagnyukova, T. V, Serebriiskii, I. G, Zhou, Y, Hopper-Borge, E. A, Golemis, E. A, & Astsaturov, I. (2010) Chemotherapy and signaling: How can targeted therapies supercharge cytotoxic agents? *Cancer biology & therapy* **10**, 839–53.
7

[50] Alam, A. (2018) Chemotherapy treatment and strategy schemes: a Review. *Journal of Toxicology* **2**.
7

[51] Kim, J. Y, Cho, C. H, & Song, H. S. (2017) Targeted therapy of ovarian cancer including immune check point inhibitor. *Korean Journal of Internal Medicine* **32**, 798–804.
8

[52] Mittica, G, Ghisoni, E, Giannone, G, Genta, S, Aglietta, M, Sapino, A, & Valabrega, G. (2018) PARP Inhibitors in Ovarian Cancer. *Recent Patents on Anti-Cancer Drug Discovery* **13**, 392–410.
8

[53] Drerup, J. M, Liu, Y, Padron, A. S, Murthy, K, Hurez, V, Zhang, B, & Curiel, T. J. (2015) Immunotherapy for Ovarian Cancer. *Current Treatment Options in Oncology* **16**, 1–20.
8

[54] National Cancer Institute. (2018) Radiation therapy. *NCI Dictionary of Cancer Terms*.
8

[55] Shen, D.-W, Pouliot, L. M, Hall, M. D, & Gottesman, M. M. (2012) Cisplatin resistance: a cellular self-defense mechanism resulting from multiple epigenetic and genetic changes. *Pharmacological reviews* **64**, 706–21.
9

[56] Sullivan, R. J & Flaherty, K. T. (2011) BRAF in Melanoma: Pathogenesis, Diagnosis, Inhibition, and Resistance. *Journal of skin cancer* **2011**, 423239.
9

[57] Gottesman, M. M. (2002) Mechanisms of Cancer Drug Resistance. *Annual Review of Medicine* **53**, 615–627.
9

[58] Holohan, C, Van Schaeybroeck, S, Longley, D. B, & Johnston, P. G. (2013) Cancer drug resistance: An evolving paradigm. *Nature Reviews Cancer* **13**, 714–726.
9

[59] Zahreddine, H & Borden, K. L. B. (2013) Mechanisms and insights into drug resistance in cancer. *Frontiers in Pharmacology* **4**, 28.
9

[60] Holzer, A. K, Manorek, G. H, & Howell, S. B. (2006) Contribution of the major copper influx transporter CTR1 to the cellular accumulation of cisplatin, carboplatin, and oxaliplatin. *Molecular Pharmacology* **70**, 1390–1394.
9

[61] Choi, C.-H. (2005) ABC transporters as multidrug resistance mechanisms and the development of chemosensitizers for their reversal. *Cancer cell international* **5**, 30.
9, 10

[62] Montoni, A, Robu, M, Pouliot, É, & Shah, G. M. (2013) Resistance to PARP-Inhibitors in Cancer Therapy. *Frontiers in Pharmacology* **4**, 18.
10

[63] Ganoth, A, Merimi, K. C, & Peer, D. (2015) Overcoming multidrug resistance with nanomedicines. *Expert Opinion on Drug Delivery* **12**, 223–238.
10, 11

[64] Tredan, O, Galmarini, C. M, Patel, K, & Tannock, I. F. (2007) Drug Resistance and the Solid Tumor Microenvironment. *JNCI Journal of the National Cancer Institute* **99**, 1441–1454.
10

[65] Rivankar, S. (2014) An overview of doxorubicin formulations in cancer therapy. *Journal of Cancer Research and Therapeutics* **10**, 853.
10

[66] Weiss, R. B. (1992) The anthracyclines: will we ever find a better doxorubicin? *Seminars in oncology* **19**, 670–86.
10

[67] Choi, C.-H. (2005) ABC transporters as multidrug resistance mechanisms and the development of chemosensitizers for their reversal. *Cancer cell international* **5**, 30.
10

[68] Hoelder, S, Clarke, P. A, & Workman, P. (2012) Discovery of small molecule cancer drugs: successes, challenges and opportunities. *Molecular oncology* **6**, 155–76. 11

[69] Yang, X, Feng, Y, Gao, Y, Shen, J, Choy, E, Cote, G, Harmon, D, Zhang, Z, Mankin, H, Hornicek, F. J, & Duan, Z. (2015) NSC23925 prevents the emergence of multidrug resistance in ovarian cancer in vitro and in vivo. *Gynecologic Oncology* **137**, 134–142. 11

[70] Sun, X & Hu, B. (2018) Mathematical modeling and computational prediction of cancer drug resistance. *Briefings in bioinformatics* **19**, 1382–1399. 12

[71] Zhao, B, Hemann, M. T, & Lauffenburger, D. A. (2016) Modeling Tumor Clonal Evolution for Drug Combinations Design. *Trends in Cancer* **2**, 144–158. 12, 13, 14

[72] Dean, A. M, Lehman, C, & Yi, X. (2017) Fluctuating Selection in the Moran. *Genetics* **205**, 1271–1283. 12

[73] Moran, P. A. P. (1958) Random processes in genetics. *Mathematical Proceedings of the Cambridge Philosophical Society* **54**, 60. 13

[74] Fisher, R. A. (1999) *The genetical theory of natural selection*. (Oxford University Press), p. 318. 13

[75] Wright, S. (1931) Evolution in Mendelian Populations. *Genetics* **16**, 97–159. 13

[76] Kimmel, M & Axelrod, D. E. (2002) *Branching Processes in Biology*. (Springer-verlag New York) Vol. 19. 13, 24

[77] Haeno, H, Gonen, M, Davis, M. B, Herman, J. M, Iacobuzio-Donahue, C. A, & Michor, F. (2012) Computational modeling of pancreatic cancer reveals kinetics of metastasis suggesting optimum treatment strategies. *Cell* **148**, 362–375. 15

[78] Bozic, I, Antal, T, Ohtsuki, H, Carter, H, Kim, D, Chen, S, Karchin, R, Kinzler, K. W, Vogelstein, B, & Nowak, M. A. (2010) Accumulation of driver and passenger mutations during tumor progression. *Proceedings of the National Academy of Sciences of the United States of America* **107**, 18545–50. 15

[79] Traina, T. A & Norton, L. (2011) Log-Kill Hypothesis. *Encyclopedia of Cancer* pp. 2074–2075. 15

[80] Goldie, J. H & Coldman, A. J. (1998) *Drug resistance in cancer : mechanisms and models*. (Cambridge University Press). 15

[81] Norton, L & Simon, R. (1986) The Norton-Simon hypothesis revisited. *Cancer treatment reports* **70**, 163–9. 16

[82] Bonadonna, G, Zambetti, M, Moliterni, A, Gianni, L, & Valagussa, P. (2004) Clinical Relevance of Different Sequencing of Doxorubicin and Cyclophosphamide, Methotrexate, and Fluorouracil in Operable Breast Cancer. *Journal of Clinical Oncology* **22**, 1614–1620. 16

[83] Bentele, M, Lavrik, I, Ulrich, M, Stösser, S, Heermann, D. W, Kalthoff, H, Krammer, P. H, & Eils, R. (2004) Mathematical modeling reveals threshold mechanism in CD95-induced apoptosis. *The Journal of cell biology* **166**, 839–51. 17, 19

[84] Snowden, T. J, van der Graaf, P. H, & Tindall, M. J. (2017) Methods of Model Reduction for Large-Scale Biological Systems: A Survey of Current Methods and Trends. *Bulletin of mathematical biology* **79**, 1449–1486.
17

[85] Poleszczuk, J, Hahnfeldt, P, & Enderling, H. (2015) Therapeutic implications from sensitivity analysis of tumor angiogenesis models. *PloS one* **10**, e0120007.
17

[86] Zi, Z. (2011) Sensitivity analysis approaches applied to systems biology models. *IET Systems Biology* **5**, 336–346.
18

[87] McKay, M. D, Beckman, R. J, & Conover, W. J. (2000) A comparison of three methods for selecting values of input variables in the analysis of output from a computer code. *Technometrics* **42**, 55–61.
18

[88] Marino, S, Hogue, I. B, Ray, C. J, & Kirschner, D. E. (2008) A methodology for performing global uncertainty and sensitivity analysis in systems biology. *Journal of Theoretical Biology* **254**, 178–196.
19

[89] Lebedeva, G, Sorokin, A, Faratian, D, Mullen, P, Goltsov, A, Langdon, S. P, Harrison, D. J, & Goryanin, I. (2012) Model-based global sensitivity analysis as applied to identification of anti-cancer drug targets and biomarkers of drug resistance in the ErbB2/3 network. *European Journal of Pharmaceutical Sciences* **46**, 244–258.
19

[90] Zheng, Y & Sriram, G. (2010) Mathematical modeling: Bridging the gap between concept and realization in synthetic biology. *Journal of Biomedicine and Biotechnology* **2010**.
19

[91] Lu, J, Engl, H. W, & Schuster, P. (2006) Inverse bifurcation analysis: application to simple gene systems. *Algorithms for molecular biology : AMB* **1**, 11.
19

[92] Csikász-Nagy, A, Battogtokh, D, Chen, K. C, Novák, B, & Tyson, J. J. (2006) Analysis of a generic model of eukaryotic cell-cycle regulation. *Biophysical Journal* **90**, 4361–4379.
19

[93] Novak, B & Tyson, J. J. (1997) Modeling the control of DNA replication in fission yeast. *Proceedings of the National Academy of Sciences* **94**, 9147–9152.
19

[94] Efeyan, A & Serrano, M. (2007) p53: Guardian of the genome and policeman of the oncogenes.
25

[95] Rivlin, N, Brosh, R, Oren, M, & Rotter, V. (2011) Mutations in the p53 Tumor Suppressor Gene: Important Milestones at the Various Steps of Tumorigenesis. *Genes & cancer* **2**, 466–74.
25

[96] Molina, J. R & Adjei, A. A. (2006) The Ras/Raf/MAPK Pathway, Technical report.
25

[97] Chee, J. L, Saidin, S, Lane, D. P, Leong, S. M, Noll, J. E, Neilsen, P. M, Phua, Y. T, Gabra, H, & Lim, T. M. (2013) Wild-type and mutant p53 mediate cisplatin resistance through interaction and inhibition of active caspase-9. *Cell Cycle* **12**, 278–288.
25

[98] Hientz, K, Mohr, A, Bhakta-Guha, D, & Efferth, T. (2017) The role of p53 in cancer drug resistance and targeted chemotherapy. *Oncotarget* **8**, 8921–8946.
25

[99] Zhang, T, Brazhnik, P, & Tyson, J. J. (2007) Exploring mechanisms of the DNA-damage response: p53 pulses and their possible relevance to apoptosis. *Cell Cycle* **6**, 85–94. 25

[100] Keng, B. W & Aguda, B. D. (2006) Akt versus p53 in a network of oncogenes and tumor suppressor genes regulating cell survival and death. *Biophysical Journal* **91**, 857–865. 25

[101] Gillespie, D. T. (1977) Exact stochastic simulation of coupled chemical reactions. *The Journal of Physical Chemistry* **81**, 2340–2361. 26

[102] Rich, J. T, Neely, J. G, Paniello, R. C, Voelker, C. C, Nussenbaum, B, & Wang, E. W. (2010) A practical guide to understanding Kaplan-Meier curves. 28

[103] Kishore, J, Goel, M, & Khanna, P. (2010) Understanding survival analysis: Kaplan-Meier estimate. *International Journal of Ayurveda Research* **1**, 274. 29

[104] Hientz, K, Mohr, A, Bhakta-Guha, D, & Efferth, T. (2017) The role of p53 in cancer drug resistance and targeted chemotherapy. *Oncotarget* **8**, 8921–8946. 30

[105] Essmann, F & Schulze-Osthoff, K. (2012) Translational approaches targeting the p53 pathway for anti-cancer therapy. *British journal of pharmacology* **165**, 328–44. 30

[106] Zhao, Y, Yu, H, & Hu, W. (2014) The regulation of MDM2 oncogene and its impact on human cancers. *Acta Biochimica et Biophysica Sinica* **46**, 180–189. 30

[107] Chow, L. M & Baker, S. J. (2006) PTEN function in normal and neoplastic growth. *Cancer Letters* **241**, 184–196. 30

[108] Galluzzi, L, Senovilla, L, Vitale, I, Michels, J, Martins, I, Kepp, O, Castedo, M, & Kroemer, G. (2012) Molecular mechanisms of cisplatin resistance. *Oncogene* **31**, 1869–1883. 32

[109] Galluzzi, L, Vitale, I, Michels, J, Brenner, C, Szabadkai, G, Harel-Bellan, A, Castedo, M, & Kroemer, G. (2014) Systems biology of cisplatin resistance: past, present and future. *Cell death & disease* **5**, e1257. 32

[110] Shelling, A. N. (1997) Role of p53 in drug resistance in ovarian cancer. *Lancet* **349**, 744–5. 32

[111] Giannakeas, V, Sopik, V, & Narod, S. A. (2016) A model for ovarian cancer progression based on inherent resistance. *Gynecologic Oncology* **142**, 484–489. 37

[112] Schwarz, R. F, Ng, C. K. Y, Cooke, S. L, Newman, S, Temple, J, Piskorz, A. M, Gale, D, Sayal, K, Murtaza, M, Baldwin, P. J, Rosenfeld, N, Earl, H. M, Sala, E, Jimenez-Linan, M, Parkinson, C. A, Markowetz, F, & Brenton, J. D. (2015) Spatial and Temporal Heterogeneity in High-Grade Serous Ovarian Cancer: A Phylogenetic Analysis. *PLOS Medicine* **12**, e1001789. 37

[113] Yu, G, Li, N, Zhao, Y, Wang, W, & Feng, X. L. (2018) Salidroside induces apoptosis in human ovarian cancer SKOV3 and A2780 cells through the p53 signaling pathway. *Oncology Letters* **15**, 6513–6518. 40

[114] Hientz, K, Mohr, A, Bhakta-Guha, D, & Efferth, T. (2017) The role of p53 in cancer drug resistance and targeted chemotherapy. *Oncotarget* **8**, 8921–8946. 40